El-Neelain University
Faculty of Engineering
Department of Control Engineering
Master of Science in Control Engineering

Dual Axis Sun Tracking Control Utilizing Fuzzy Fractional Order PID Controller

التحكم في المتتبع الشمسي في محورين بإستخدام المتحكم التناسبي التكاملي التفاضلي ذو الرتبة الكسرية الغامض

A Thesis Submitted in Partial Fulfillment of the Requirements of the Master Degree in Control Engineering

Prepared By:

Zain Elabedin Mohamed Elamin Ahmed

Supervised By:

Dr. Ibrahim Mohamed Hafiz Abdelltif Sanhoury

October, 2020

DEDICATIONS

This study is lovingly dedicated to my parents for their support, my brothers, my sisters and my friends whose has been constant source of inspiration for me.

They have given me the drive and discipline to tackle any task with enthusiasm and determination.

Without their love and support, this research would not have been made possible.

ACKNOWLEDGEMENT

I wish to express my profound gratitude to my Supervisor Dr. **Ibrahim Mohamed Hafiz Abdullatif Sanhoury** for his valuable guidance, continues encouragement, worthwhile suggestions and constructive ideas throughout this research. His support, pragmatic analysis and understanding, made this study a success and knowledgeable experience for me.

ABSTRACT

The solar power is the most important clean renewable power, which is mainly found in hot climate countries. The technology helped to produce electricity from solar power, But the obstacle that faces producing the maximum amount of electricity from the Sun, is the apparent movement of the Sun that makes it change its position. The objective of this research is to design a solar tracking system to harness the maximum solar irradiance. The solar tracking system is the most appropriate method to improve the efficiency of solar cells by tracking the Sun with respect to its change in direction. The purpose of a similar approach is used to track the Sun movement from North to South over the period of a year. This research proposes fuzzy fractional order PID (FFOPID) controller for a dual-axis solar tracking Photovoltaic (PV) system. The controller maintains the maximum power from PV solar cells through tracking Sunlight to be incident perpendicularly to the PV panel. The dynamic models for solar radiation, solar panel and electro mechanics system were obtained. Furthermore, the proposed controller is verified through simulation work utilizing SIMULINK/MATLAB. Moreover, the results represent the behavior of solar cell while solar radiation changes and there is a variation in temperature during simulation run time. The proposed controller is benchmarked with Fractional Order PID and conventional PID controllers. It's fond that, the proposed controller achieves better results to get maximum power the solar Dual Axis system. Furthermore, the proposed controller has faster tracking response via 9.6% than PID and via 6.5% FOPID controllers.

مستخلص

الطاقة الشمسية هي أهم طاقة متجددة نظيفة توجد بشكل رئيسي في البلدان الحارة. ساعدت التكنولوجيا كثيرا في إنتاج الكهرباء من الطاقة الشمسية. لكن العقبة التي تواجه إنتاج أكبر قدر من الكهرباء من الشمس هي طبيعة الحركة الظاهرية للشمس التي تجعلها تغير موقعهاباستمرار. الهدف من هذا البحث هو تصميم نظام تتبع شمسي للاستفاده من أقصى قدره للإشعاع الشمسي. يعد نظام التتبع الشمسي الطريقة الأنسب لتحسين كفاءة الخلايا الشمسية من خلال تتبع الشمس فيما يتعلق بتغير اتجاهها. الغرض من استخدام هذا النهج هو تتبع حركة الشمس من الشمال إلى الجنوب خلال فترة عام. يقترح هذا البحث تصميم وحدة تحكم غامضة تناسبية تكاملية تفاضلية ذات رتبة كسرية لنظام فولت ضوئي مزدوج المحور لتتبع الطاقة الشمسية. تهدف وحدة التحكم إلى زيادة كفاءة الخلايا الكهروضوئية الشمسية عن طريق تتبع ضوء الشمس للسقوط بشكل عمودي على اللوحة الكهروضوئية في جميع الأوقات. يتكون النظام من لوحة شمسية كهروضوئية يُسمح لها بالتحرك باستخدام محركين ووحدة تحكم. كمرحلة تصميم أولى ، تم الحصول على النماذج الديناميكية للإشعاع الشمسي والألواح الشمسية والنظام الكهروميكانيكي من خلال برنامج الماتلاب ، وتم محاكاة النظام ، وكذلك محاكاه سلوك الخلية الشمسية عند تغير الإشعاع الشمسي وانخفاض درجة الحرارة الساقطة عليها. ولزيادة كفاءة النظام تمت دراسة العديد من وحدات التحكم مثل وحدة المتحكم التناسبي نتيجة هذا البحث أن المتحكم المقترح له استجابة .وتم ضبط معاملاتها ذو الرتبة الكسرية التكاملي التفاضلي أسرع من المتحكم التناسبي التكاملي التفاضلي التقليدي بنسبه 9.6% و المتحكم التناسبي التكاملي التفاضلي ذو الرتبة الكسرية بنسبه 6.5%.

TABLE OF CONTENTS

CHAPTER THREE

MODELING AND CONTROLING OF DUAL AXIS SUN TRACKING

CHAPTER FOUR

SIMULATION AND RESULTS

CHAPTER FIVE

CONCLUSION AND RECOMMENDATIONS

LIST OF FIGURES

LIST OF TABLES

LIST OF ABBREVIATIONS

AI	Artificial Intelligent
ANN	Artificial Neural Network
D	Derivative
DC	Direct Current
FC	Fractional Calculus
FFOPID	Fuzzy Fractional Order PID controller
FLC	Fuzzy Logic Controller
FOC	Fractional Order Control
FOPID	Fractional Order PID controller
GA	Genetic Algorithm
I	Integral
LED	Light Emitted Diode
MMF	Magnetic Motive Force
NL	Negative large
NM	Negative Medium
NS	Negative Small
P	Proportional
PID	Proportional Integral Derivative
PL	Positive large
PM	Positive Medium
PS	Positive Small
PSO	Particle Swarm Optimization
PV	Photo voltaic
ZO	Zero

LIST OF SYMBOLS

k_P	Proportional gain
k_i	Integral gain
k_d	Derivative gain
Ti	Integral time
Td	Derivative time
T	Motor torque
i	Armature Current
Kt	Torque constant
e	Electromotive force
$\dot{\theta}$	Angular velocity of the shaft
Kp	Electromotive force constant
K	Motor torque and back EMF constant
J	The moment of inertia of the rotor
b	The motor viscous friction constant
La	Electric inductance
Ra	Electric resistance
V	Voltage source
Kg	Gears ratio
θ	Servo gear angle
I_{ph}	Photo cell current
I_{sc}	Current in shunt resistance
I_o	Diode reverse saturation current
I_D	Diode current
I_{cell}	PV cell terminal current
I_{rr}	reverse saturation current
T_r	Reference temperature
R_s	Series resistance
R_{sc}	Shunt resistance

N_s	Number of series cell
N_p	Number of parallel cells
μ	fractional derivative
λ	fractional integration
V_{OC}	open-circuit voltage
V_g	band gap voltage
V_D	diode voltage
V_{cell}	PV cell terminal voltage
P_{MPP}	maximum power point
q	electron charge

CHAPTER ONE
INTRODUCTION

1.1 Background

Significant progress has been made over the last few years in the research and development of renewable energy systems such as wind, sea wave and solar energy systems [1], [2]. Among the energy resources, solar energy is considered nowadays as one of the most reliable, daily available and environmentally friendly renewable energy sources. Currently the use of PV cells increased and the needs for solar tracker gained interest among researchers due to the fact that the efficiency of the solar system can be improved if a proper tracking system is used [1].

Photovoltaic (PV) cells gained much attention as a clean energy source. The main idea of using PV cells is to produce an electrical energy out of the solar energy. This energy can be used in many applications, such as heating, lighting and operating different electric and electronic devices. Higher efficiency of such system can be achieved when the Sunlight is perpendicular to the surface of the PV solar panel, consequently maximum possible electrical energy can be produced [2].

The tracking for PV solar panel can be done manually or automatically. In manual tracking approach, the PV panel is oriented manually at the beginning of each season to a predetermined angle. For automatic tracking method, the PV panel is mounted on a single-axis or dual-axis tracking mechanism and is controlled to track the Sun ray's trajectory during the day [3].

A solar tracking system is a control system that consists of several sensors which check the perpendicular of the Sunlight to the PV panel, and a controller that give signals to one or more actuators to move the panel to the right position. If one actuator is used the system is a single degree of freedom, in the other hand, multiple degrees of freedom system increases the efficiency of the PV panel. In case of two-axis trackers the panel is positioned to track the orientation of the maximum Sun light throughout the day by adjusting the tracker angles [3].

The daily average output of the PV cells can be enhanced by a solar tracker. Many research works had been implemented on single axis solar tracker systems because single axis trackers are cheap and easy to implement. However, when accuracy and performance are concerned, dual axis solar trackers could give a better result [3].

1.2 Problem Statement

Most of the solar cells are fixed in one position to face the Sun. In this case it is difficult to get the maximum power from the solar cell. Many research works have been made the solar cell panel track the Sun to get the maximum power output. The controllers that used to let the solar cell panel track the Sun had fixed parameters, which degrades the performance in achieving the maximum power form the solar cell.

1.3 Objectives

The main objectives of this dissertation are:

1. Obtain mathematically model of the Dual axis Sun tracking system.
2. Propose Fuzzy Fractional Order PID controller (FFOPID) to enhance the performance of the solar system.
3. Verify the effectiveness of the proposed controller via simulation work.

1.4 Scope of Study

The scope of study of this research is given as follows:

1. Obtain the mathematical model of Dual axis Sun tracker.
2. Obtain the mathematical model of PV cell.
3. Utilize the proposed (FFOPID) controller to get maximum power from the Solar system.
4. Benchmark the result of the proposed controller with Fractional Order PID controller (FOPID) and PID controller.
5. Simulate the work through MATLAB/Simulink.
6. Verify the effectiveness of the proposed controller via various simulation works.

1.5 Dissertation outline

The outlines of this dissertation are given as follows:

Chapter two presents literature review of previous works, introduces the dual axis solar tracking system. Moreover, the chapter illustrates servo motor fundamentals and different types of controllers are then presented. Chapter three presents the derivation for mathematical model of the Dual Axis solar tracking system model and the PV cell model. Chapter four shows simulation results and discussion of the dual axis solar tracker system within the proposed (FFOPID) controllers and benchmark with the PID and FOPID controllers. Chapter five gives the conclusion of this research and recommendations for the future work.

CHAPTER TWO
LITERATURE REVIEW

2.1 Introduction

This chapter will show the previous studies in the field of Solar tracking systems. Also, it will discuss the Solar system, Solar panel construction and it will illustrate the tracking techniques. Moreover, it will review some types of control methods used to keep dual axis Sun tracking give high performance such as the PID, FOPID and FFOPID controllers.

2.2 The previous works

In the literature, different designs for solar tracking can be found. In [4], the authors designed a mechanical passive solar tracker activated by bimetallic strips and controlled by viscous damper. They developed the analytical model and performed a computer simulation in addition to the experimental verification through a prototype. In [5], the introduction of the theoretical aspects associated with the design of a single vertical axis tracking system, taking into consideration shadowing between different trackers and back-tracking features. The main idea in their work is to optimize the spacing between adjacent trackers. In [6], the authors presented a single axis three position Sun tracking PV module, that can adjust the PV position only at three fixed angles (three position tracking: morning, noon and afternoon). The efficiency of such system can be improved if continuous tracking throughout the daylight is performed.

Many research works had been proposed to maximize the power from the PV panel. In [7], presented a two-axis solar tracker, which is controlled using both PID and fuzzy controller. The system consists of two DC motors used to rotate the two axes of the PV cell. In [8], the authors developed a fuzzy logic controller for a maximum power point tracking of a standalone PV system. They compared the performance of the fuzzy logic controller with the conventional PI controller. They showed that the fuzzy logic approach developed better and faster tracking capabilities for different optimum operating points. In [9], the authors investigated a maximum power point tracking method based on fuzzy cognitive networks. They presented the efficiency of the algorithm for identifying the maximum operating point for the real time maximum power point tracking control of the PV modules. The controller was off-line trained using appropriately constructed data in order for the controller to operate with any PV system under changing climate conditions. Moreover, it presented a design and experimental implementation of a maximum power point tracker for photovoltaic systems.

2.3 Solar System

Solar tracking system sets either a Solar panel (photo-voltaic) or a concentrating solar reflector towards the Sun while tracking the position of the Sun. It gained importance mainly since the source of solar energy is free to provide the electrical energy and heat. There are some factors that affecting the Solar tracking system, which are the natural climatic condition of the place where the system is to be used, the load of the system, the availability of the Solar tracking of the system [10].

2.3.1 Solar Cells

A Solar cell also called a photo voltaic cell is an electrical device that converts the energy of light directly into electricity through the photo voltaic effect. It is a form of photoelectric cell, defined as a device whose electrical characteristics like current, voltage and resistance are varied when exposed to light; cells can be described as photo voltaic even when the light source is not necessarily Sunlight like lamplight and artificial light [11].

2.3.2 A Solar Panel

A Solar panel is a set of solar photo voltaic modules that electrically connected and mounted on a supporting structure. A photo voltaic module is a package that connected and assembled based on the Solar cells. The Solar module can be used as a component of a larger photo voltaic system to generate and supply electricity in commercial and residential applications. Each module is rated by its DC output power under the standard test conditions, which typically ranges from 100 to 320 watts. A single Solar module can produce a limited amount of power; most installations contain multiple modules. A photo voltaic system typically includes a panel or an array of solar modules, an inverter, and sometimes a battery and Solar tracker [11].

2.3.3 Theory and construction Solar Modules

Solar modules used light energy (photons) from the Sun to generate electricity through the photo voltaic effect. The majority of modules use wafer based crystalline silicon cells or thin-film cells based on cadmium luridness or silicon. The structural (load carrying) member of a module can either be on the top layer or the back layer. Cells must be protected from mechanical damage and moisture. Most Solar modules are rigid, but semi-flexible ones are available, based on thin-film cells. These early Solar modules were first used in space in 1958 [11].

2.3.4 The photo voltaic effect

The photo voltaic effect is the creation of voltage or electric current in a material upon exposure to light. The standard photo voltaic effect is directly related to the photoelectric effect, though their different processes. When the Sunlight is incident upon a material surface, the electrons present in the valence band absorb energy and, being excited, jump to the conduction band and become free. These highly excited, non-thermal electrons diffuse, and some reach a junction where they are accelerated into a different material by a built-in potential (Galvani potential). This generates an electromotive force, and thus some of the light energy is converted into electric energy. The photo voltaic effect can also occur when two photons are absorbed simultaneously in a process called two-photon photo voltaic effect. Figure 2.1. Shows how PV technology work [11]

.

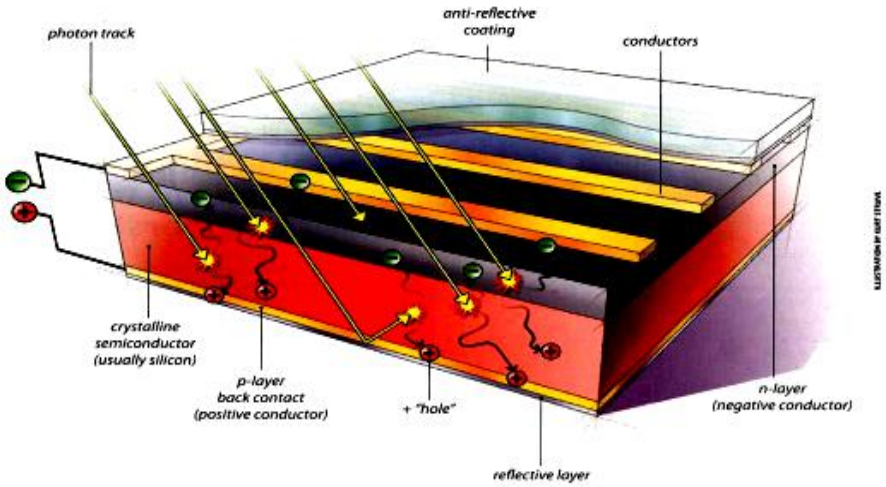

Figure 2.1: PV technology work

2.4 Tracking Techniques

There are two types of tracking techniques which are fixed programmable control technique and dynamic tracking technique. The main difference between both techniques is the way of tracking the movement of the Sun. For fixed programmable control technique, the positions of the Sun at different times were predetermined by the programmer based on a real time clock system. The system operated with designated programming algorithms without any feedback signals. In contrast, dynamic tracking technique tracked the locations of the Sun's during the day where the decisions were influenced by feedback signals from sensors or GPS modules.

2.4.1 Types of Tracker Actuator Driver

Two main types of actuator drivers commonly used in Solar tracking system for detecting or locating the Sun. Those are the electronic (active) tracker and mechanical (passive) tracker.

2.4.1.1 Electronic (Active) Tracker

Electronic tracker or commonly name as active utilized electronic sensor or transducer that able to detect the intensity of light such as Light Dependent Resistor (LDR) or photo diode linked to one or more motors for pivoting the position of the Solar panel to minimize the angle between the line of the Sun and a face perpendicular to the panel. Those sensors be placed on the trackers at certain spots to prevent any disturbances. Some of the active trackers were designed with an electro-mechanical system drives and other type of actuators. They are used due its higher efficiency and reliability as compared with trackers without an electro-mechanical system. Figure 2.2 shows an active tracker [11]

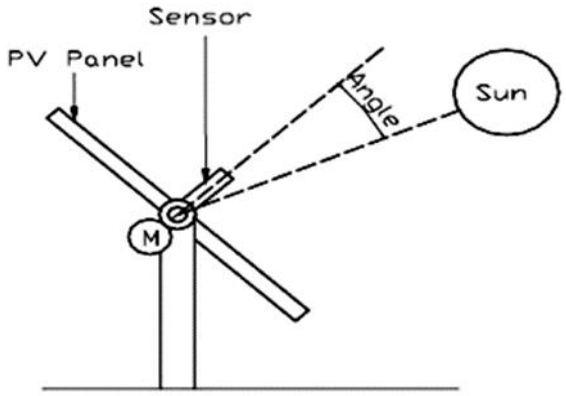

Figure2.2: An Active Solar tracker

2.4.1.2 Mechanical (Passive) Tracker

A mechanical or passive tracker manipulated the Sun's radiation to heat up the gases to produce forces to move the tracker. It used two identical containers (each at either side of the panel and equal distance from the central of the Solar panel which are filled with a liquid under partial pressure. Then the tracker is placed with side of the tracker faced on the Sun while the Sun heats the fluid causing the liquid to vaporize thus increased the pressure inside the container. Hence, the tracker balances the Solar panel at a certain slope. This system is simple and cheap and the maintenance is free, but it gives less efficiency and need an extra supervision since the tracker rarely locating perpendicularly and difficult to cope with the changes of the movement of the Sun. Furthermore, the trackers faced significant problems during the cloudy days where the Sun apparently appeared behind the clouds where the tracker will lose sight of the Sun. As a result, the temperature will fluctuate while the gas inside the container will expand and compress in an impropriate way. However, passive trackers can be relatively low-cost in the way of increasing the output power of a solar array in areas with less cloud. Based on Figure 2.3, the tracker should

be placed by facing the PV panel starting from the west since the Sunrise is from east where the Sun radiation will heat the un-shaded west-side of the container. It will force the liquid into the shaded eastside of the container, hence it changes the balance of the tracker and it will swing to the east [11].

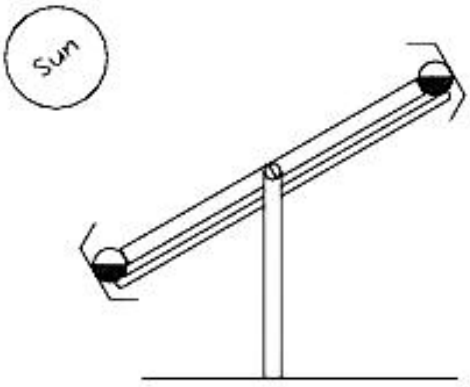

Figure 2.3: A Passive Solar Tracker

2.4.2 Type of Solar Tracker Axis

There are two main types of solar tracker axis which are single axis and double axis trackers.

2.4.2.1 Single Axis Tracker

There are two types of single axis tracker which can be either in vertical axis or horizontal axis. Any countries in the tropical region should deploy horizontal type of tracker since the Sun normally positioned at the highest point. Meanwhile, the vertical type will be used by other country if the Sun position is low most of the time and has high altitudes, or the duration of summer day is longer. Figure 2.4 and Figure 2.5 shows example of single axis trackers [12].

Figure 2.4: A Horizontal Single Axis Solar Tracker

Figure 2.5: A Vertical Single Axis Solar Tracker

2.4.2.2 Dual Axis Tracker

A dual axis tracker is a tracker that has two degrees of freedom which acts as axes of rotation in the horizontal and vertical axis. The vertical axis pivot shaft allows the tracker to move to a compass point such as east to west while the horizontal axis works as elevation that moves depending on the altitude of the Sun. Hence this system is able to tracks the Sun's movement in any positions either east to west or north to south. This system should be operated under a computer control according to the expected solar position and need to be calibrated with tracking sensor to control motors that oriented the panels toward the Sun. Therefore, this system allows the increase of power output energy compared to the fixed panels [12].

2.5 Servo Motors

Servomotor and has high torque capabilities. Unlike large industrial motors, Servomotors are used for precise speed and precise position control at high torques. Their basic principle of operation is the same as that of other electromagnetic motors. However, their construction, design and mode of operation are different. Their power ratings vary from a fraction of a Watt up to a few 100 Watts. Due to their low inertia; Servomotors have high speed of response. That is why Servomotors are smaller in diameter but longer in length. Servomotors operate at very low speeds. Servomotors have wide application in radar, tracking and guidance systems, process controllers [13].

2.5.1 DC Servomotors

DC Servomotors either separately excited DC motors or permanent magnet DC motors. The schematic diagram of a separately-excited DC motor along with its armature and field magnetic motive forces (MMFs)are shown in Figure 2.6 [13].

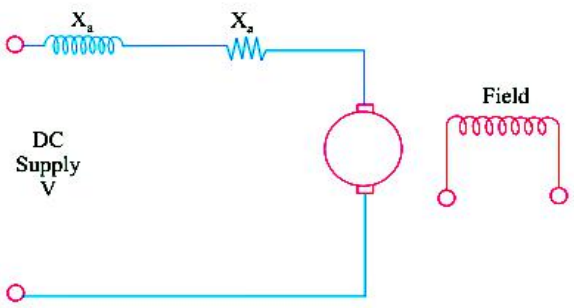

Figure 2.6: The schematic diagram of a separately-excited DC motor

The speed of DC Servomotors is controlled by varying the armature voltage. Their armature is deliberately designed to have large resistance such that torque speed characteristics are linear and have a large negative slope, the torque/speed characteristics are shown in Figure 2.7 [13].

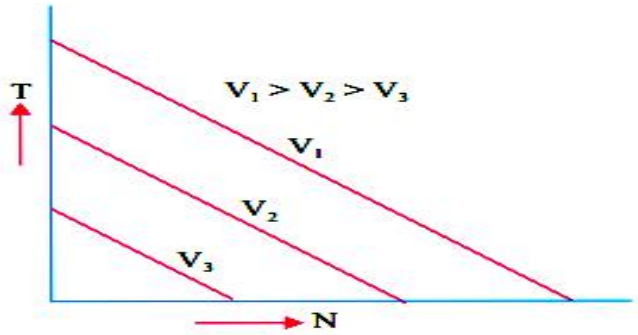

Figure 2.7: Torque/speed characteristics

2.6 Proportional Integral Derivative (PID) Controller

A proportional integral derivative (PID) controller is a control loop feedback mechanism (controller) widely used in industrial control systems. A PID controller calculates an error value as the difference between a measured process variable and a desired set point. The controller attempts to minimize the error by adjusting the process through use of a manipulated variable.

The PID controller algorithm involves three separate constant parameters. The proportional(P), the integral(I) and derivative(D) values, as shown is Fig2.8 denoted P, I, and D. P depends on the present error, based on the accumulation of past errors, and D is a prediction of future errors, based on current rate of change. The weighted sum of these three actions is used to adjust the process via a control element such as the position of a control valve, a damper, or the power supplied to a heating element, Table 2.1 shows the effect of increasing a parameter independently

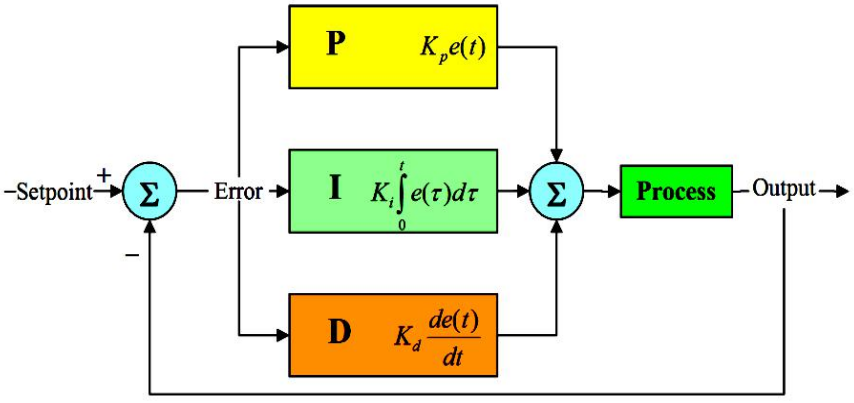

Figure 2.8: Proportional Integral Derivative (PID)

Table 2.1: Effects of increasing a parameter independently

Parameter	Rise time	Overshoot	Settling time	Steady-state
k_p	Decrease	Increase	Small change	Decrease
k_i	Decrease	Increase	Increase	Eliminate
k_d	No change	Decrease	Decrease	Small effect

2.6.1 Tuning of Proportional Integral Derivative controller

The process of selecting the controller parameters to meet given performance specifications is known as controller tuning. There are several methods for tuning a PID loop. The most effective methods involve the development of some form of process model, and then choosing P, I, and D based on the dynamic model parameters.

If a mathematical model of the plant can be derived, then it is possible to apply various design techniques for determining parameters of the controller that will meet the transient and steady-state specifications of the closed-loop system. However, if the plant is so complicated that its mathematical model cannot be easily obtained, then an analytical or computational approach to the design of a PID controller is not possible. The experimental approaches are used for tune the PID controllers [14]

There are many methods used to tune of the PID controller such as: Manual tuning, Ziegler-Nichols, Tyreus luyben and Cohen-coon.

2.7 Fuzzy Logic Controller (FLC)

Fuzzy Logic Controller (FLC) is one of the most popular new technologies in artificial intelligent (AI).Which is defined as a combination of control theory, operations research, and artificial intelligence (AI).

Conventional set theory distinguishes between elements that are members of a set and are not, there being very, clear or crisp boundaries. In a fuzzy set all the elements of the universe have been named and supplemented to a number between 0and 1. This number demonstrates to what degree this generic element belongs to the defined fuzzy set. Actually, according to this definition added to every element a number which constitutes the membership degree of this element. Actually, a fuzzy set is given by its membership function. The value of this function determines if the element belongs to the fuzzy set and in what degree [15].

2.7.1 The Basics of Fuzzy Logic

A fuzzy control is a controller that is intended to manage some vaguely known or vaguely described process. The controller can be used with the process in two modes:

i. Feedback mode when the fuzzy controller acts as a control device.
ii. Feed forward mode where the controller can be used as a prediction device.

The illustrates of the basic components of fuzzy logic controller, as shown is Figure (2.9) [17].

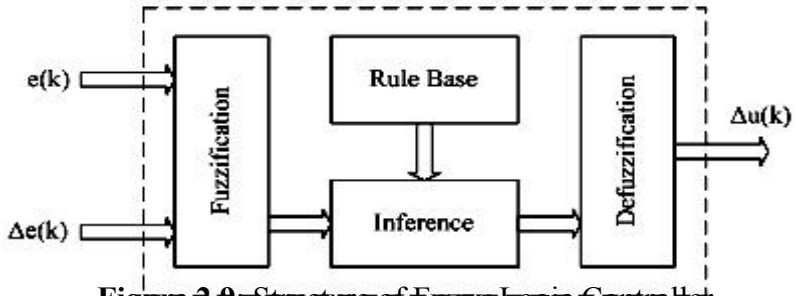

Figure 2.9: Structure of Fuzzy Logic Controller

The plant output is denoted by $\Delta u(k)$, the plant input is denoted by $e(k)$, and the reference input to the fuzzy controller is denoted by $\Delta e(k)$.

The fuzzy controller has four main components, which are [15]:

- **Fuzzification**

The first block of the fuzzy controller is fuzzification, which converts each piece of input data to degrees of membership by a look up in one or several membership functions. The fuzzification block thus matches the input data with the conditions of the rules to determine how well the condition of each rule matches that particular input instance. There is a degree of membership for each linguistic term that applies to that input variable.

- **Inference mechanism**

Inference mechanism or engine is the processing program in a fuzzy control system. It derives a conclusion from the facts and rules contained in the knowledge base using various human expert techniques.

- **Rule-base**

A group of rules may use several variables both in the condition and the conclusion of the rules. They are based on a set of rules that a human expert would follow in diagnosing a problem.Rule-base also where the knowledge is stored.

- **Defuzzification**

Defuzzification is a process that maps a fuzzy set to a crisp set and has attracted far less attention than other processes involved in fuzzy systems and technologies. Four most common defuzzification methodicalness membership method, Center of gravity method, Weight average method, Mean –maximum membership method.

2.8 Fractional Calculus

The history of the Fractional Calculus (FC) covers over three hundred years, similar to that of classical differential calculus. In last two decades, the FC has become much popular among the researchers of different streams. Fractional calculus was not much popular earlier because of its highly complex mathematical expressions. But with the development of computational technologies it has become possible to deal with fractional calculus. Fractional calculus is an extension of integer order calculus in which ordinary differential equations have been replaced by fractional order differential equations. In fractional order differential equations, derivatives and integrals are not necessarily of integer order and they span a wider range of differential equations. Fractional calculus deals with fractional integration and differentiation. Therefore, a generalized differential and integral operator has been introduced as a single fundamental operator represented by where *a* and *t* denote the two integration limits related to the operation of the fractional differentiation, and is the order of fractional differentiation or integration. Positive indicates differentiation and negative indicates integration [16].

2.8.1 Fractional Order PID Controller

Fractional Order Control (FOC) means controllers described by fractional order differential equations. Recently, there are increasing interests to enhance the performance of ordinary PID controller by using the concept of fractional calculus, where the orders of derivatives and integrals are non-integer. The idea of fractional order controller was first proposed by A.Oustaloup, through Commando Robuste d'Ordre Non-Entire (CRONE) controller in 1991. Later on, Igor Podlubny [17] had initiated the most common form of fractional order PID in the form of PIλDμ in 1999 involving an integrator of order λ and differentiator of order μ. Clearly, depending on the values of the orders λ and μ, the numerous choices for the controller's type can be made. It is better as compared to the conventicler PID controller. One of the most important advantages of the FOPID controller is the better control of dynamical systems, which are described by fractional order mathematical models. Another advantage lies in the fact that the FOPID controllers are less sensitive to changes of parameters of a controlled system. This is due to the two extra degrees of freedom to better adjust the dynamical properties of a fractional order

control system. However, up till now there is no systematic way to set the value for λ and μ. The fractional integrator-differential equation of the FOPID controller is given by [17]:

$$u(t) = k_P e(t) + k_I {D_t}^{-\lambda} e(t) + k_D {D_t}^{\mu} e(t) \quad (2.3)$$

The transfer function of the FOPID controller is obtained through Laplace transform as follows:

$$G_{FOPID}(s) = \frac{U(s)}{E(s)} = k_p + \frac{k_i}{s^{\lambda}} + k_d\, s^{\mu} \quad (2.4)$$

Where *E(s)* is an error and *U(s)* is controller's output. It is obvious that the fractional order PID controller not only needs design three parametersk_p, $k_i$andk_d, but also design two orders λ and μ of integral and derivative controllers. Figure 2.9 shows the block diagram configuration of the FOPID controller [19].

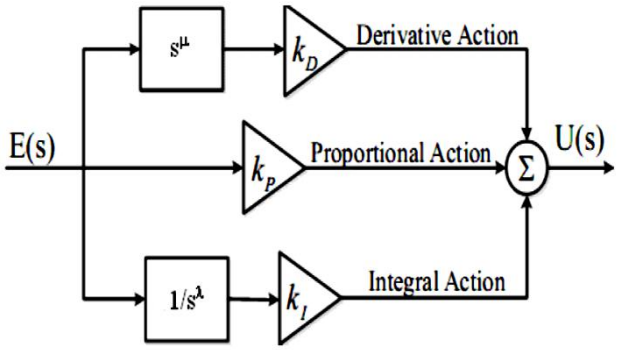

Figure 2.10: Block diagram of the FOPID controller

Figure 2.11 depicts the FOPID controller and explains how the order of the integrator and the order of the differentiated can vary versus the horizontal and vertical axis. The fractional order PID controller generalizes the ordinary integer order PID controller and expands it from point to plane. This expansion could provide much more flexibility in ordinary PID controller design [17].

2.9 Summary

This chapter shows some studies in the field of Sun tracking system. Also, it discusses the Solar system, Solar panel construction and it illustrates the tracking techniques. Addition to that, it presents some types of control methods such as the PID, FOPID and FFOPID controllers.

CHAPTER THREE

MODELING AND CONTROLING OF DUAL AXIS SUN TRACKING

3.1 Introduction

This chapter presents the modeling of dual axis Sun tracker and the design of proposed controller applied to the system to improve the response. Moreover, its presents PV cell model. Furthermore, the chapter illustrates PID controller and fractional order PID controller approach. Moreover, fuzzy fractional order PID controller is proposed such that the controller parameters are been time-varying.

3.2 Structure of Dual Axis Sun tracking system

Solar energy is a way of converting Sun's rays into useful electrical or heat energy. To obtain electrical energy photo voltaic (PV) cells are used. The efficiency of cells varies depending on their types and technology used for manufacturing. Solar energy is gaining popularity due to it being sustainable and available abundantly in form of Sun's rays. Output efficiency of PV cells is not very. However, the efficiency could be increased if PV cell is aligned with Sunrays. To increase the efficiency, Solar tracking systems are used which is an electro-mechanical system that ensures Sun's radiation remain perpendicular to PV cell throughout the day.

PV cell efficiency could be increased by three methodologies . The first approach tries to increase the output efficiency of PV cell. The second method uses efficient control algorithms such as maximum power point (MPP) tracking to increase output power. The third algorithm adopts different types of Solar trackers to increase the output power [18].

In this research, a dual axis Solar tracking system frame work is presented as shown in Figure 3.1. The azimuth and tilt angle are controlled by DC servo motors. The DC servo motors is controlled by FOPID controller and the parameters of the controller are selected via Fuzzy algorithm such that the parameters will be varying with time.

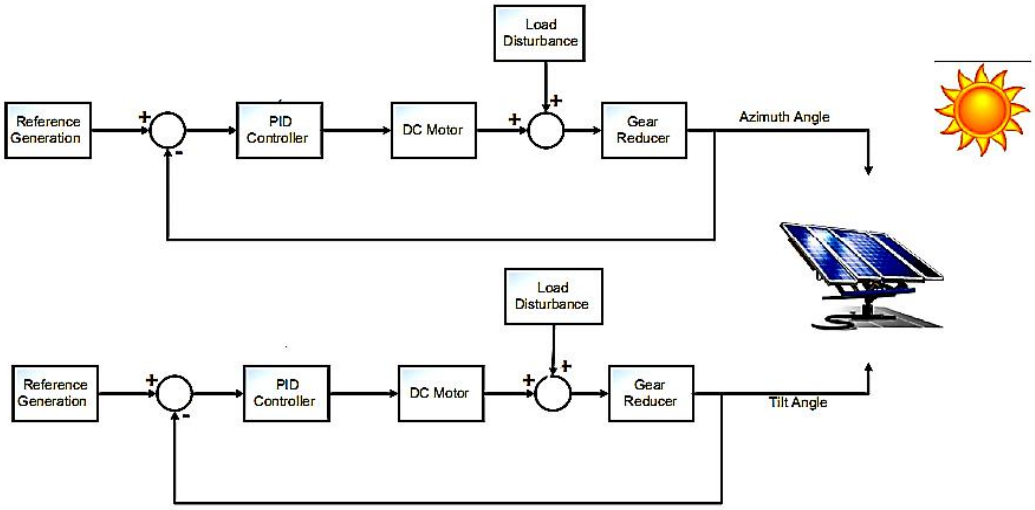

Figure 3.1: Dual Axis Sun tracking system

The control algorithms position the panel from east to west along the apparent path of the Sun and north-south positioning in the changing seasons of the year, as shown in Figure 3.2 [18].

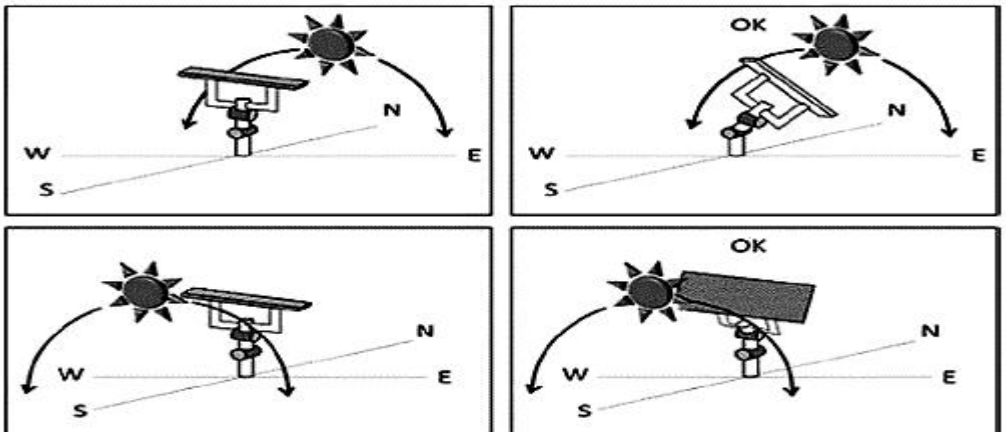

Figure 3.2: Positions of the Sun and Solar panel

The Solar tracker system requires movement in different directions, and uses electric motors as actuator. In Solar tracking system design, any light sensitive device can be used as input sensor unit to detect and track the Sun position, based on sensors readings, and generates Sun tracking error. The control unit produces the voltage used to command the circuit to drive the motor. The rotational displacement of the motors make the Solar panel track the Sun. Simplified block diagram representation of Solar tracking system is shown in Figure 3.3 [18].

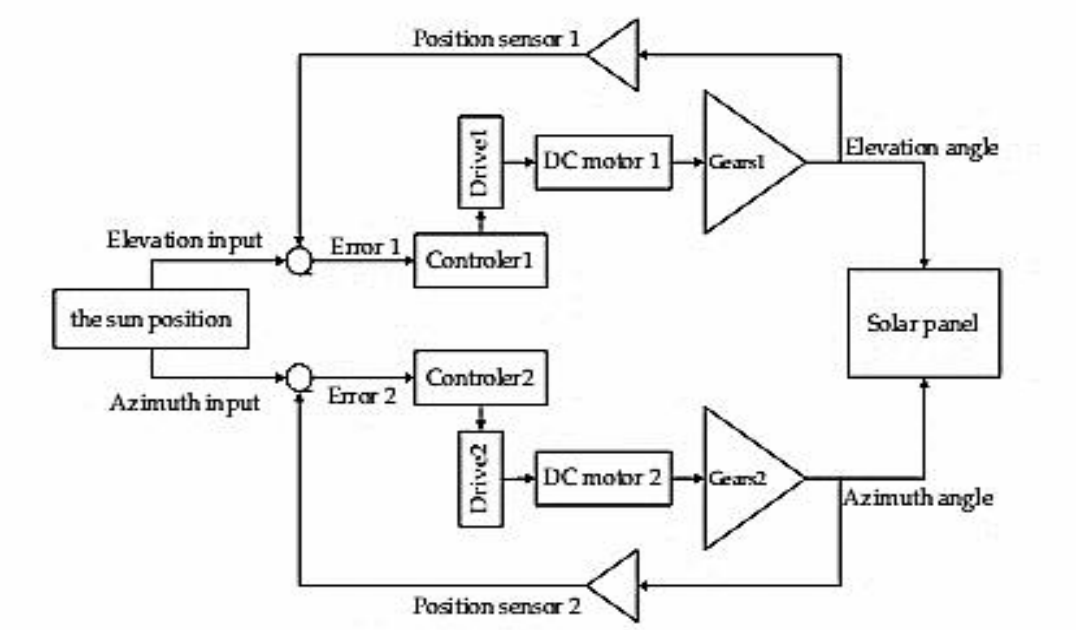

Figure 3.3: Design of the control system at the PV system of two Axis Solar tracking

3.3 Mathematical model of the Dual Axis Sun tracking system

The mathematical model of the Dual Axis Sun tracking system involves the model of DC servomotors for both axes. Considered same types of motors for both axis and develop model accordingly. The block diagram of DC motor is shown in Figure 3.4.

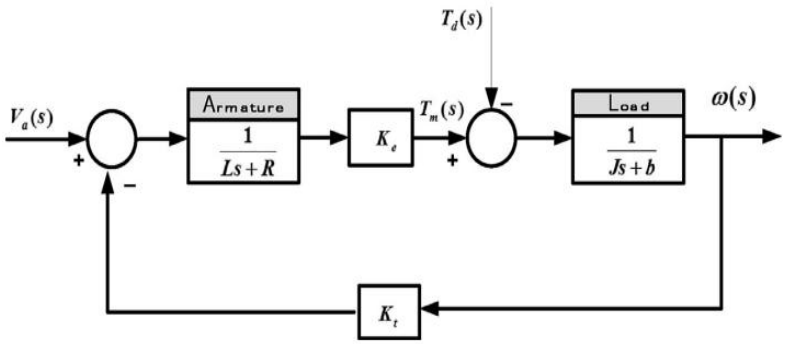

Figure 3.4: DC Servo motor block diagram

The torque generated by DC motor is proportional to the armature current and the strength of the magnetic field. Assume that the magnetic field is constant and, therefore, the motor torque (T) is proportional to only the armature current (i) by a constant factor (K_t) called torque constant as shown in the Equation (3.1). This is referred to as an armature-controlled motor.

$$T = K_t\, i \tag{3.1}$$

The back electromotive force emf (e) is proportional to the angular velocity of the shaft ($\dot{\theta}$) by a constant factor (K_b) called electromotive force constant as shown in the Equation (3.2).

$$e = K_b\dot{\theta} \tag{3.2}$$

In system international units, the motor torque and back emf constants are equal, that is, $K_t = K_b$; therefore, (k) will be used to represent both the motor torque constant and the back emf constant.

By using the following governing equations based on Newton's 2^{nd} law in Equation (3.3)

$$J\ddot{\theta} + b\dot{\theta} = Ki \tag{3.3}$$

And Kirchhoff's voltage law in Equation (3.4).

$$La\frac{di}{dt} + Ra * i = V - K\theta * b \tag{3.4}$$

Where $J$the moment of inertia of the rotor is, b is the motor viscous friction constant, L_a is the electric inductance R_a is the electric resistance, and V is the voltage source. By applying the Laplace transform, the modeling equations can be expressed in terms of the Laplace variables as follows.

$$s(Js + b)\theta(s) = KI(s) \tag{3.5}$$

$$(L_a s + R_a)I_{(s)} = V_{(S)} - Ks\theta_{(S)} \tag{3.6}$$

Subsisting the value of $I(s)$from (3.5) into (3.6), and get the open loop transfer function as follows:

$$G(s) = \frac{\dot{\theta}(s)}{V(s)} = \frac{K}{(Js+b)(Las+Ra)+K^2} \ [\frac{rad/sec}{V}] \tag{3.7}$$

In model (3.7), the transfer function is velocity and in the Solar panel system, the position is desired. Therefore, the position can be obtained through integration both side of (3.7) yields:

$$\frac{\theta(s)}{V(s)} = \frac{K}{s((Js+b)(Las+Ra)+K^2)} \ [\frac{rad}{V}] \tag{3.8}$$

The position $\theta(s)$ in (3.8) is the rotational displacement that applied to the motor's shaft. However, there are gears between shaft and load with ratio known as gears ratio (Kg), therefore the transfer function becomes as follows (3.9).

$$\frac{\theta(s)}{V(s)} = \frac{KKg}{s((Js+b)(Las+Ra)+K^2)}\left[\frac{rad}{V}\right] \tag{3.9}$$

The physical parameters of the servo motor used for simulation purpose are given in Table 3.1.

Table 3.1: DC servo motor parameter [13]

K_t	0.01125 N.m/A
K_b	0.0125 V/rad/s
Ra	6.25Ω
J	1e-6 kg.m^2/rad
B	0.000001 N.m/rad/s

3.4 PV Panel Model

The PV panel model is the single-diode model, this model represents the illuminated solar cell in its simplest form as a PN junction, as shown in Figure 3.5.

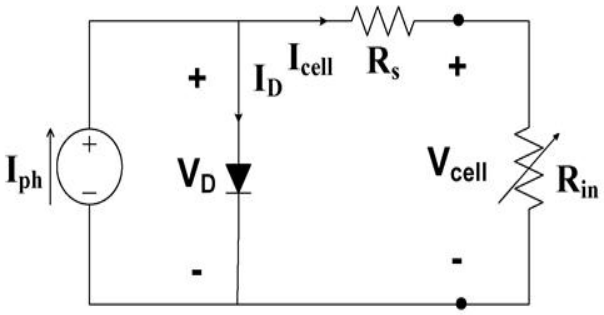

Fig 3.5: The single-diode model

$$V_{cell} = V_D - I_{cell}R_S \tag{3.10}$$

$$I_{cell} = I_{ph} - I_D = I_{ph} - I_o\,(e^{Kp_v}\,(V_{pv} + I_{pv}R_a)\,\text{-}1) \tag{3.11}$$

WhereV_{cell}andI_{cell} arethe PV cell terminal voltage and current, V_D and I_D are the diode voltage and current, K_p =q/pkT with the electron charge q=1.6*10^{-2}, k is the Boltzmann's constant, T is the cell temperature, and p=1.3 is the ideal p-n junction characteristic factor for mono crystalline Solar cells. I_{ph} is the photo current given by

$$I_{ph} = (I_{sc} + K_T(T + T_r))\,\frac{\lambda}{100} \tag{3.12}$$

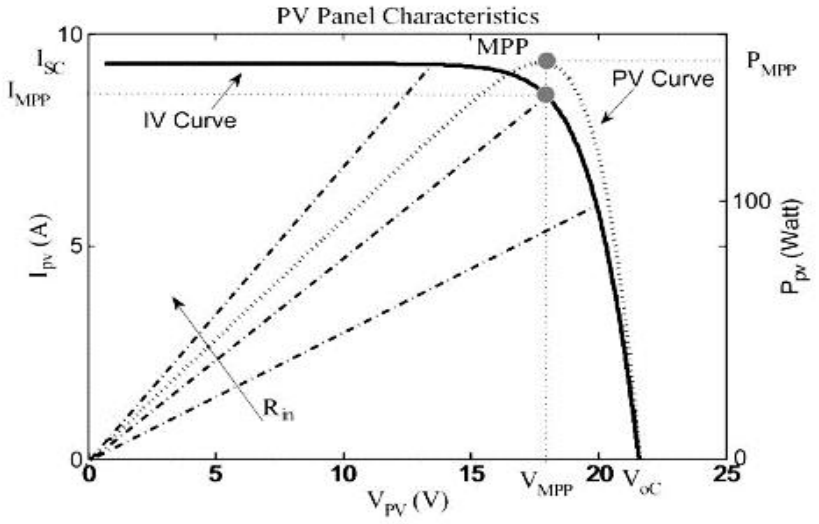

Fig 3.6: PV panel characteristics

Table 3.2: PV panel parameters

P_{max}	V_{max}	I_{max}	V_{oc}	I_{sc}	N_S	N_P
50 W	17.3 V	8.7 A	21.6 V	9.3 A	36	2

Where I_{sc} is the short-circuit cell current at reference temperature and insulation, *K(mA/K)* is the short-circuit current temperature coefficient, λ is the insulation in (MW/cm^2), and I_o is the saturation current in diode reverse-biased direction given as [19].

$$I_o = I_{rr}\left(\frac{T}{T_r}\right)^3 e^{\left(\frac{qV_g\left(\frac{1}{T_r}-\frac{1}{T}\right)}{pK}\right)} \quad (3.13)$$

Where I_{rr} is the reverse saturation current at the reference temperature T_r, V_g is the bandgap voltage of the semiconductor making up the cell, which equals 1.12 eV.

The PV panel model can be computed using (3.11) by taking into consideration the number of cells connected in series Ns and in parallel Ns as follows:

$$R_s = -\frac{dV}{dI_{Voc}} - \frac{1}{X_V} \quad (3.14)$$

$$X_V = I_o * \frac{q}{pKT}\left(e^{\frac{qV_{oc}}{pKT}}\right) \quad (3.15)$$

The PV panel power is computed by multiplying (3.14) and (3.15) with the PV voltage V_{panel}

$$P_{panel} = N_p I_{ph} V_{pv} - N_p I_o V_{pv}\left(e^{\left(\frac{K_{pv}(V_{pv}+I_{pv}R_S)}{Ns}\right)} - 1\right) \quad (3.16)$$

The panel *IV* and *PV* characteristics curves are obtained by plotting the *PV* current and *PV* power as a function of the *PV* voltage, as shown in Figure 3.5. Table 3.2 shows the parameters of the *PV* panel used. Moreover, Figure 3.5 illustrates the location of three important points on the *PV* panel characteristics; the short-circuit current (I_{sc}), the open-circuit voltage (V_{OC}), and the maximum power point (P_{MPP},I_{MPP} , V_{MPP}) [19].

3.5 Controllers Design

In this section the three different control methods are presented, the PID controller, Fractional order PID controller and Fuzzy Fractional order PID controller, respectively.

3.5.1 Proportional Integral Derivative (PID) Controller

The PID controller is given as follows [20] by substituting the parameters of equation (3.17)

$$PID\ (t) = K_p\ (e\ (t)) + K_i \int (e(t))dt + K_d(\frac{d(e(t))}{dt}) \quad (3.17)$$

By taking Laplace transform PID controller transfer function become:

$$C(s) = K_p + \frac{K_i}{s} + K_d * s \quad (3.18)$$

The schematic diagram for PID controller shown in Figure 3.6.

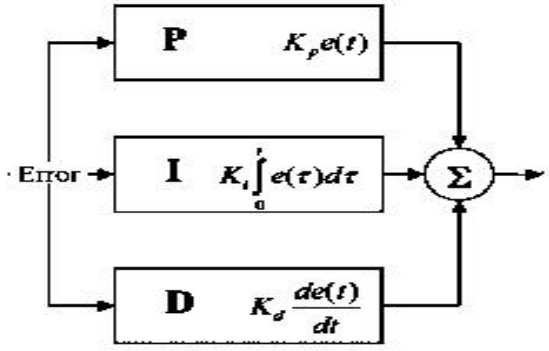

Figure 3.6: Schematic diagram for PID controller

PID controller has three terms. The proportional term (P) corresponds to proportional control. The integral term (I) give a control action that is proportional to the time integral of the zero. The derivative term (D) is proportional to the time derivative of the control error. There are many variations of the PID algorithm that will substantially improve its performance and operability [14].

3.5.2 Fractional Order PID controller

Friction order calculus offers a modern modeling approach for systems with exceptional dynamical properties by introducing the concept of a derivative of non-integer (frictional) order. In terms of applications frictional order founds its way into complex mathematical and physical problem, and it is found a useful approach in automatic control and system theory. Fractional order PID (FOPID) controller is an advanced form of PID controller, which is illustrated in Figure 3.5. The FOPID has two addition parameters, which are the order of fractional integration λ and the order of fractional derivative μ, where λ and μ are real numbers and their values is ranging between 0 to 1. In some situation these parameters are greater than one. To represent conventional PID controllers through FOPID, the value of λ and μ are set to one. The differential equation for the FOPID controller is given as follows [17].

$$u(t) = K_p e(t) + K_i \frac{1}{s^{\lambda}} e(t) + K_d s^{\mu} e(t)$$

The schematic diagram for Fractional Order PID controllers shown in Figure 3.7.

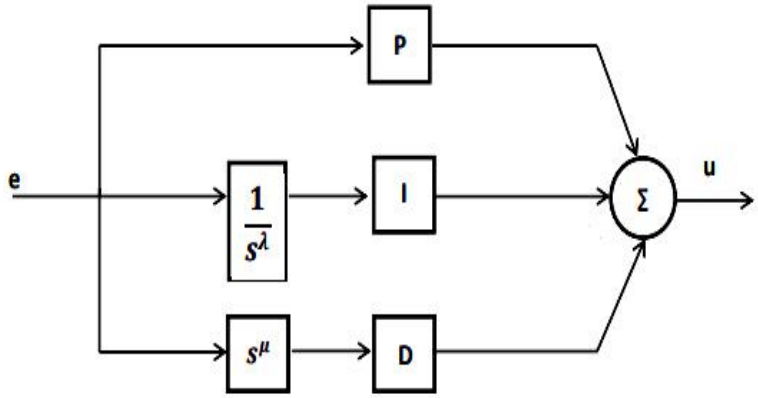

Figure 3.7: schematic diagram for Fractional Order PID controller

3.5.3 Fuzzy Fractional -Order PID Controller

A fuzzy logic controller input variable involves receiving the error signal and change of error. These variables evaluate the fuzzy control rules using the rules of inference and the appropriately computed control action is determined by using the defuzzification [17].

3.5.3.1 Fuzzification

Fuzzy fractional order PID controller the fuzzy logic uses to tune the parameters of PID in real time based on the error and change of error. The fuzzy logic chooses two fuzzy sets for the inputs (error and change of error) and three fuzzy sets for outputs (k_{ρ}, $k_i$and k_d). These Fuzzy sets consist of seven triangular membership function and seven linguistic variables as negative large (NL), negative medium (NM), negative small (NS), zero (ZO), positive small (PS), positive medium (PM) and positive large (PL). The Fuzzy sets for the inputs and outputs of FOPID controller are shown in Figures 3.8, Figure 3.9, Figure 3.10 and Figure 3.11.

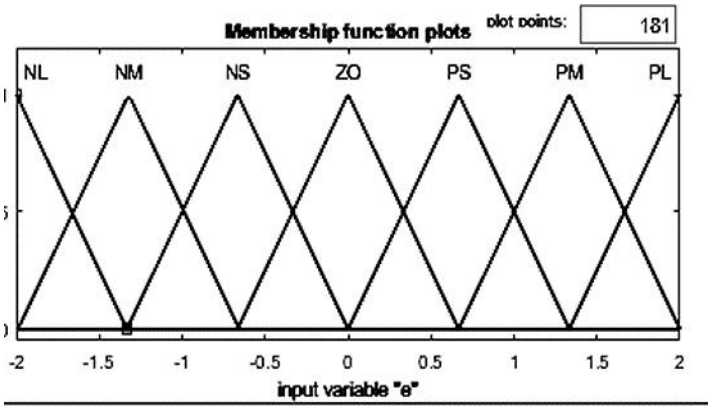

Figure 3.8: Membership function of e and *ec*

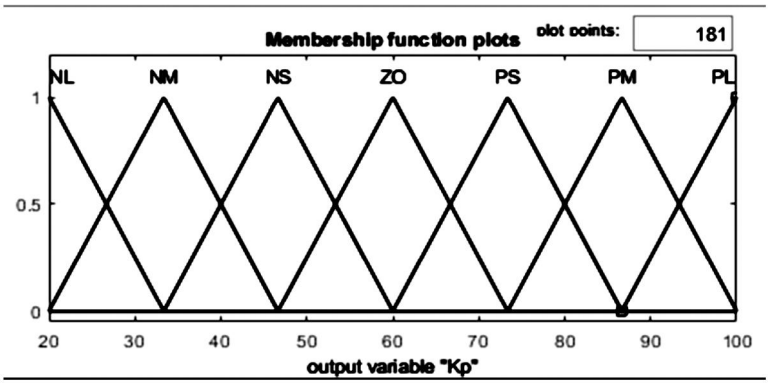

Figure 3.9: Membership function of k_p

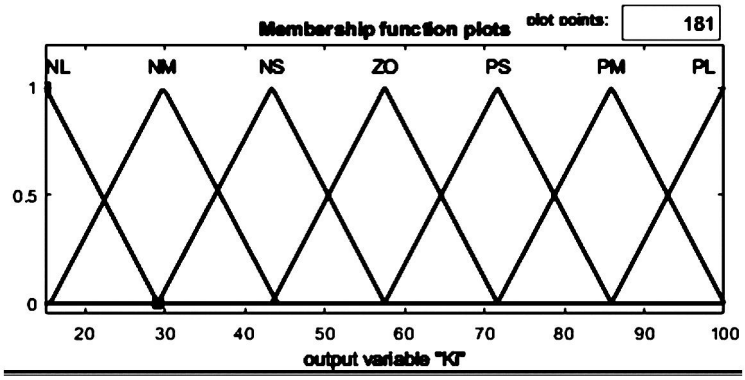

Figure 3.10: Membership function of k_i

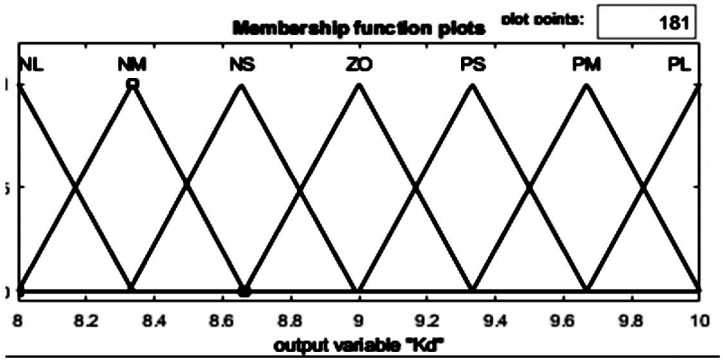

Figure 3.11: Membership function of k_d

3.5.3.2 Rule base

Rule based is a set of "if-then" statement and determines how the fuzzy logic operations are performed with the knowledge based. The tuning of PID controller parameters with time is carried out through fuzzy logic rule base that illustrated in Table 3.3.

Table 3.3: Fuzzy Rule base for parametersk_ρ, $k_i$and k_d[20]

e / *ec*	**NL**	**NM**	**NS**	**ZO**	**PS**	**PM**	**PL**
NL	PL,PS,PM	PL,PL,PS	PL,PL,ZO	PL,PL,PS	PL,PL,PS	PL,PL,PM	PL,PL,PL
NM	PL,PM,PM	PM,PS,PS	PM,PM,PS	PM,PS,PS	PM,PM,PS	PL,PL,PS	PL,PL,PM
NS	PL,PM,PS	PM,PS,PS	PS,PS,PS	PM,PS,PS	PS,PS,PS	PM,PS,PS	PL,PM,PS
ZO	PM,PM,ZO	PS,PM,ZO	PS,PM,ZO	PM,PS,ZO	PS,PM,ZO	PS,PM,ZO	PM,PM,ZO
PS	PL,PL,PS	PL,PL,PS	PM,PM,PS	PM,PS,PS	PM,PM,PS	PL,PM,PS	PL,PM,PS
PM	PL,PL,PM	PL,PL,PS	PM,PM,PS	PM,PS,PS	PM,PM,PS	PL,PL,PS	PL,PL,PM
PL	PL,PL,PL	NL,NL,PL	NL,NL,NM	NL,NM,NS	NL,NL,NS	NL,NL,NS	NL,NL,PS

From Table 3.3, if the error "*e*" is "NL" and the change in error "*ec*" is "NS", the parameters k_ρ will be positive large "PL", k_i will be positive medium "PM" and k_d will be positive small "PS". The FOPID controller parameters are tuned through the fuzzy logic to attain the best output response of the system. Only the k_ρ, k_i and k_d parameters are tuned via fuzzy logic, whereas, the parameters λ and μ keep constant. The structure of the Structure Fuzzy Fractional Order PID controller is shown in Figures 3.12.

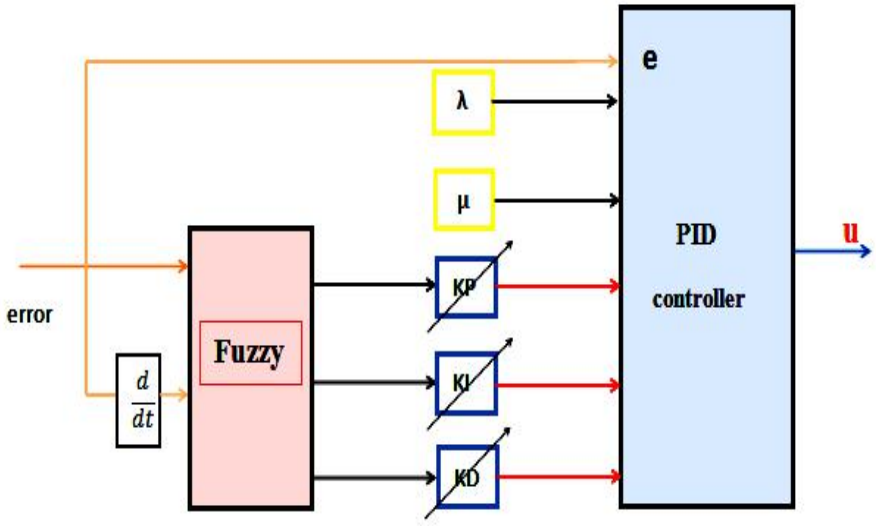

Figure 3.12: Structure Fuzzy Fractional Order PID Controller

3.6 Summary

This chapter discussed the mathematical modeling of dual axis Sun tracker and the design of the proposed controllers applied to the system. Furthermore, the model of PV cell is illustrated. Moreover, the chapter explained PID controller and illustrated how enhancement of the response of the system by using fractional order PID controller. Finally, the chapter presented the FFOPID controller to make the controller parameters varying with time.

CHAPTER FOUR

RESULTS AND DISCUSSIONS

4.1 Introduction

This chapter presents the simulation works of solar cell**.** Furthermore, the chapter shows the simulation of the dual axis Sun tracking system connected to PV model with the proposed FFOPID, FOPID and PID controllers in order to know the effectiveness of the proposed controller on the system via simulation work.

4.2 Simulation using MATLAB/Simulink

All the blocks obtained by using MATLAB/SIMULINK to represent the equations explained in previous chapter by using source, sinks and math's relation.

MATLAB/Simulink it is very straightforward to represent and then simulate a mathematical model representing a physical system. Models are represented graphically in Simulink as block diagrams. A wide array of blocks is available to the user in provided libraries for representing various phenomena and models in a range of formats. One of the primary advantages of employing Simulink for the analysis of dynamic systems that it allows us to quickly analyze the response of complicated systems that may be prohibitively difficult to analyze analytically.

4.3 Simulation of the Solar Cell

Conditions depicted in past segment are demonstrated to acquire IV and PV Characteristics of a solitary diode Sun powered cell module. The reproduction incorporates numerous subsystems: one that figures the PV cell working and reference temperature ($T\ and\ T_r$), the second ascertain I_{ph} (Photo cell current), the third one compute I_o(Diode turn around immersion current), the fourth one ascertain I_{sc}(Current in shunt resistance) while the last one figure the aggregate yield current and aggregate yield voltage (I, V).The parameters for solar cell are given in Table 4.1.

Table 4.1: Photovoltaic Model Parameters [19]

Parameters	Value
Rs	0.002(Ω)
R_{sc}	100000(Ω)
K	0.0017
I_{sc}	3.8(A)
Ns	36
Np	1
V	21.2(V)
K_i	1.381×10^{-23}(J/K)
q	1.602×10^{-19} (C)
T	25–35 –45(C° for many test)
	300 –500–700 (mW/m^{2}for many test)

4.3.1Temperature Module ($Tand T_r$)

One of the simulation blocks is the temperature (in Kelvin) is shown in Figure 4.1. The subsystem contains four blocks, the input is the operating temperature in degree centigrade and the two outputs is the temperature(T) in Kelvin and the reference temperature (T_r) is in Kelvin's. The subsystem converts the temperature units, the reference temperature assumed to be 25 C° which is room temperature, Figure 4.2 shows details of the temperature subsystem.

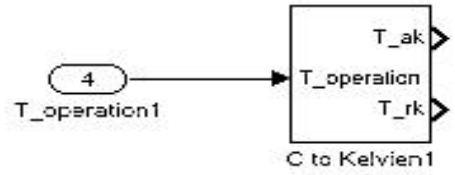

Figure 4.1: Temperature block

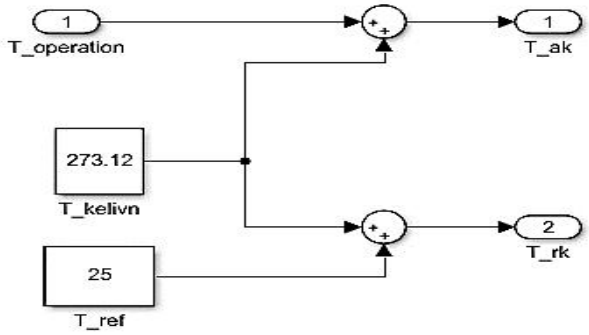

Figure 4.2: Details of the temperature subsystem

4.3.2Photo Cell Current Module (I_{ph})

This block is built from (3.13), which represents the photocell current I_{ph} as shown in Figure 4.3. The inputs are irradiance λ (mW/m^2), short circuit current I_{sc} (A), reference temperature T_r (Kelvin) and operating temperature (Kelvin) while the output is the photocell current in I_{ph}(A), the details of this block shown in Figure 4.4, which is the subsystem of the block.

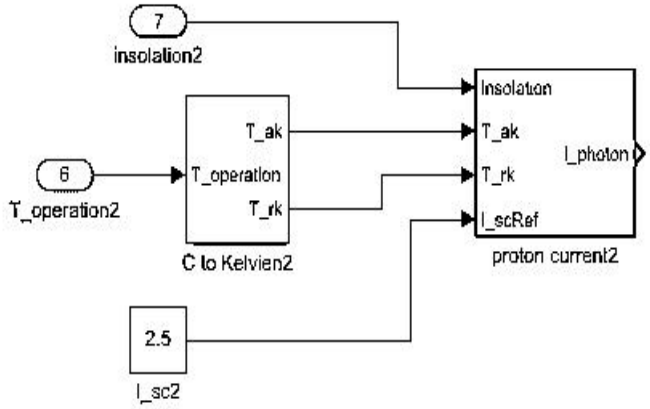

Figure 4.3: Photocell current module in the system

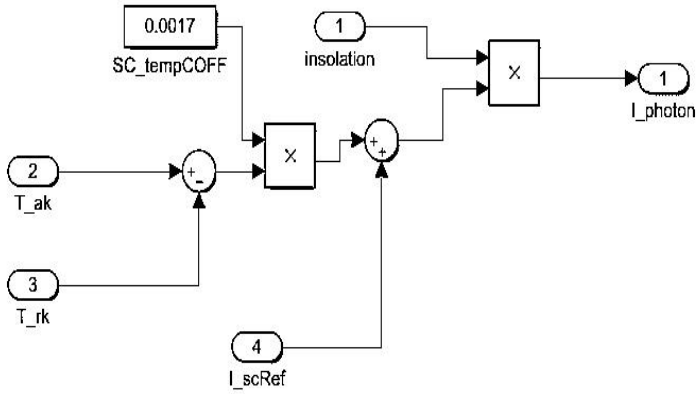

Figure 4.4: Photocell current subsystem module

4.3.4Shunt Resistance Current Module (I_{sh})

This block is based on (3.12) represents shunt resistance current I_{sh}as shown in Figure 4.5. The inputs are diode reverse saturation currentI_o (A), the temperature (T) in Kelvin and the reference temperature (T_r) in Kelvin's too. The parameters used in this block are electron charge q, Boltzmann constant K, band gap p for Silicon and diode ideality factor. The details of this block are shown in Figure 4.6.

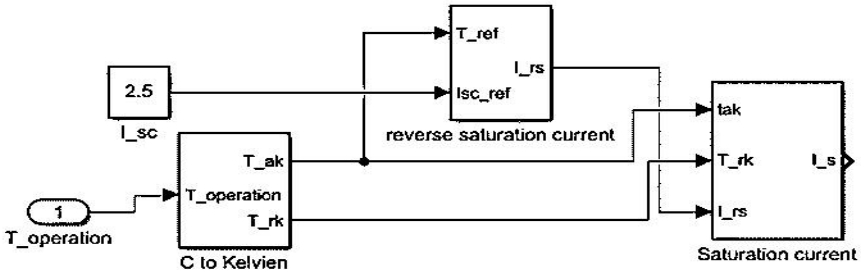

Figure 4.5: Shunt resistance current system module

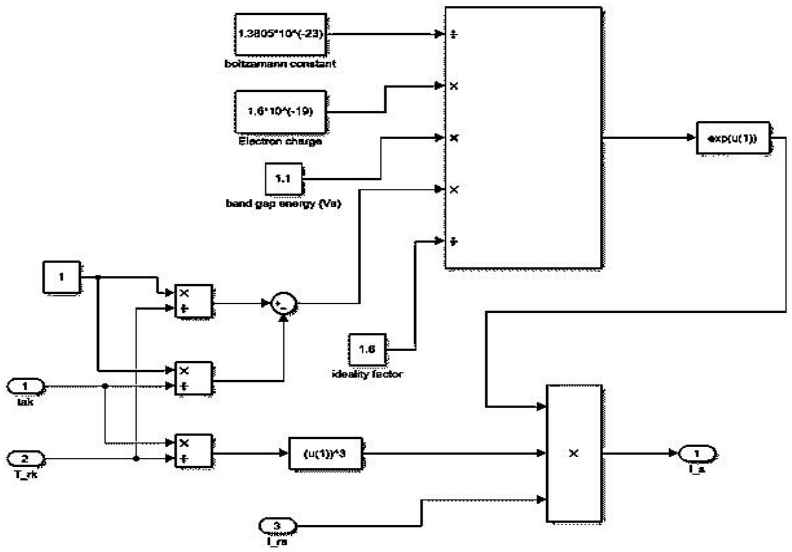

Figure 4.6: Shunt resistance current subsystem module

4.3.5 Photovoltaic Output Current Module (I_{pv})

This block built from (3.13) which represent photovoltaic output currentI_{pv}. The inputs are temperature (T) in Kelvin, short circuit current I_{sh}(A), Photocell current I_{ph}(A) and voltage across the output terminals (volt) while the outputs are photovoltaic current I_{pv} and voltage. The parameters used in this block are electron charge, Boltzmann constant, diode ideality factor, number of series cell N_s and parallel cells N_P and value of series and shunt resistanceR_{sc}. The details of this block are shown in Figure 4.7.

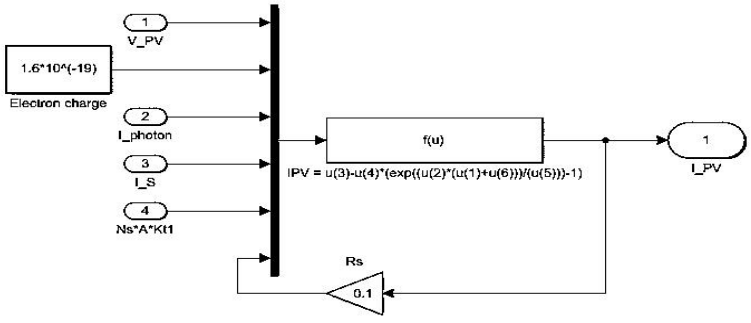

Figure 4.7: Photovoltaic current subsystem module

4.3.6 Results of Solar Cell Simulation

The simulation of solar cell specification curves I-V and P-V have been obtained for various irradiance and different operating temperature.

Figure 4.8 and Figure 4.9 shows the solar cell system module and details of the solar cell subsystem module respective.

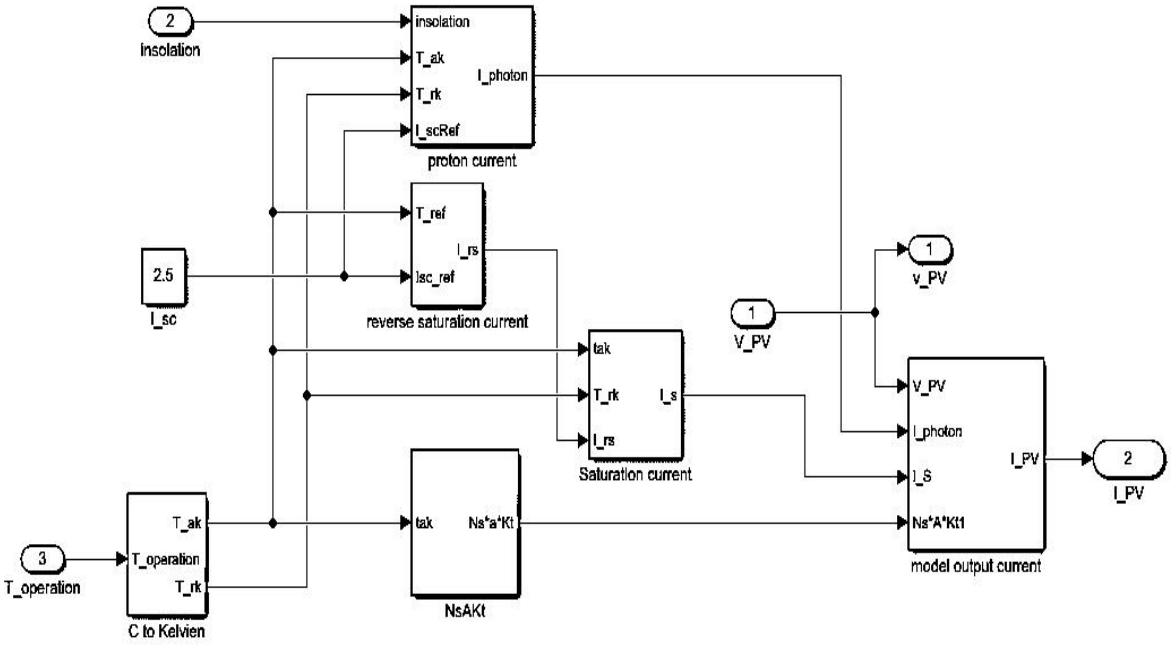

Figure 4.8: Solar cell subsystem module

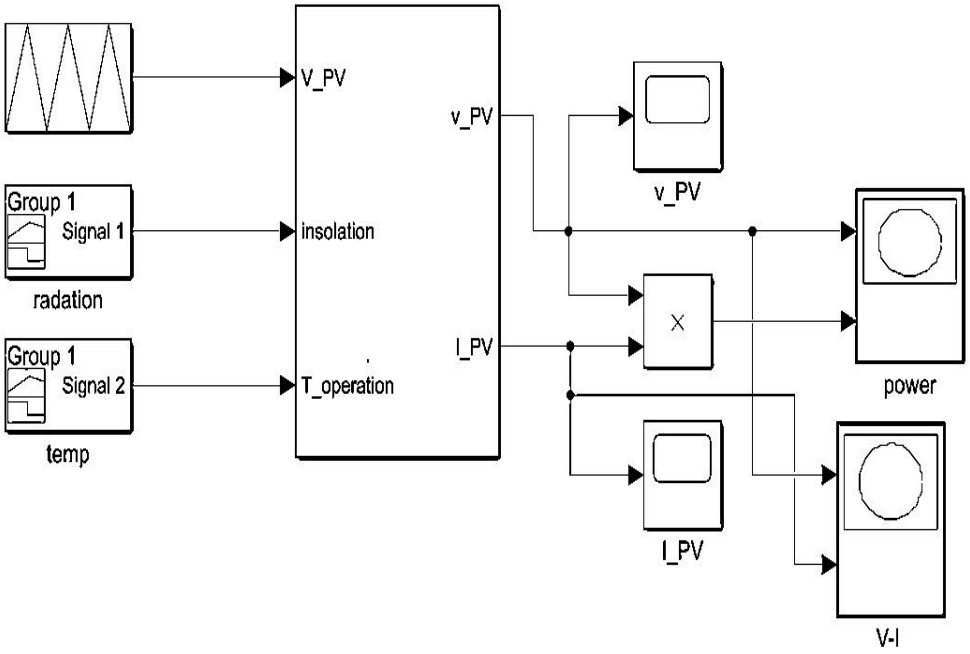

Figure 4.9: Solar cell system module

The results of solar module are obtained through using output scope block and to workspace block in MATLAB-Simulink. Figure 4.10 and Figure 4.11 shows the I-V and P-V curves for different irradiance and different temperature respective.

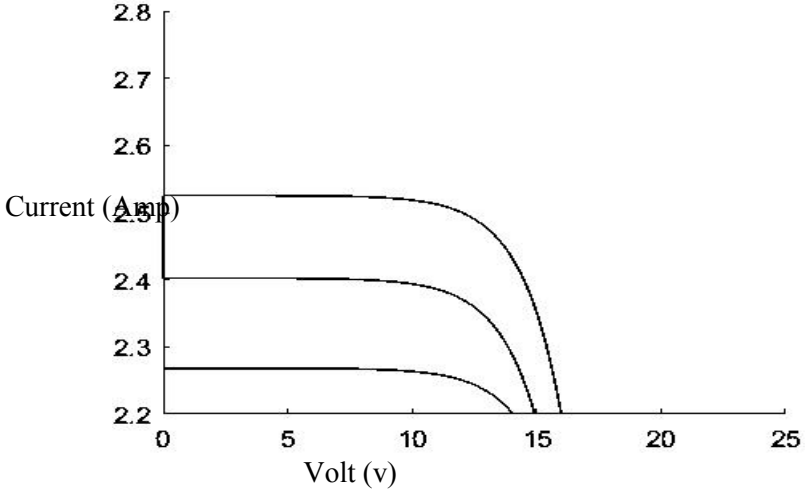

Figure 4.10: The I-V curves for different irradiance and different temperature

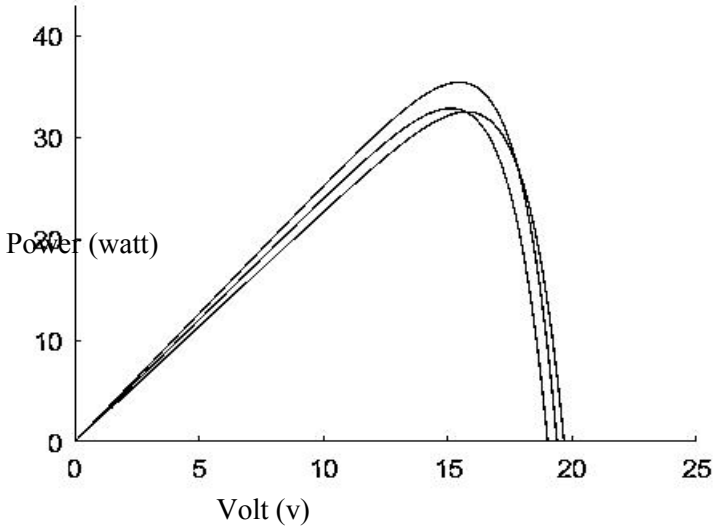

Figure 4.11: The P-V curves for different irradiance and different temperature

The I-V curves shown in Figure 4.10 represent that the effect of increasing irradiance in specified temperature is increasing the short circuit current, whereas the output voltage is not affected very much. The output voltage decreases when the operating temperature increase whiles the irradiance was constant.

The P-V curves for different irradiance and operating temperature shown in Figure 4.11, increasing the irradiance cause increasing the max power and max peak current, on the other hand increasing temperature cause to reduce the max power and max peak voltage.

4.4 Simulation of the dual axis Sun tracker

The solar tracking system (3.9) with DC servomotor and PID controller (3.18) is shown in Figure 4.12. To obtain maximum efficiency from solar panel, dual axis of Sun tracker is required, one is azimuth angle (θ) which measures the angle of incoming Sunlight to the surface of PV cell and other is tilted angle (α) which measures the inclination angle of sunlight. As Sun tracker is a non-interacting system, controller designed for single axis will be the replica for another axis also. Therefore, the analysis has been carried out on a single axis Sun tracker system as shown in Figure 4.13. Mathematical model of Sun tracker is determined using basic laws of physics (3.9) and (3.18).

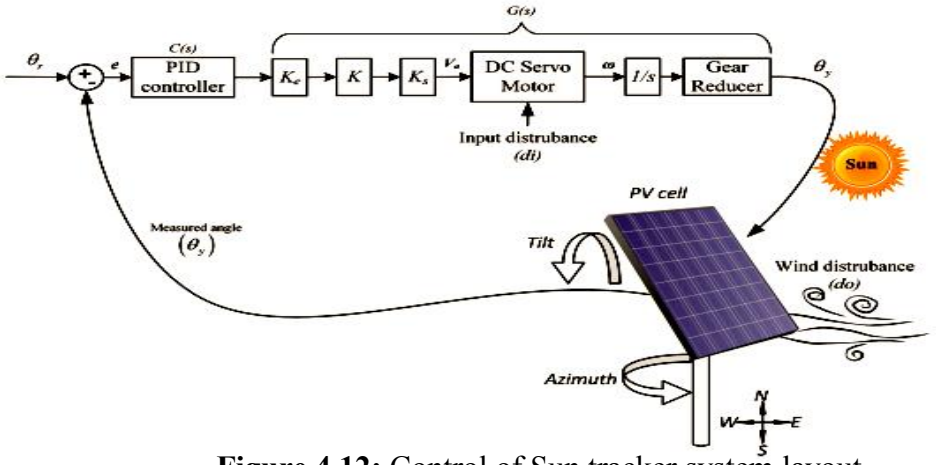

Figure 4.12: Control of Sun tracker system layout

The results for the dual axis solar tracker are presented through using PID, FOPID and FFOPID controllers. The discussion of single controller design to improve the response of the system is presented. Furthermore, dual controllers design will be obtained to get the maximum power from the solar system. Moreover, the simulation results of the dual axis Sun tracker with the proposed FFOPID controller are benchmarked with the result of the conventional PID and FOPID controllers. Figure 4.13 shows the block diagram of DC servo motor without controller [21].

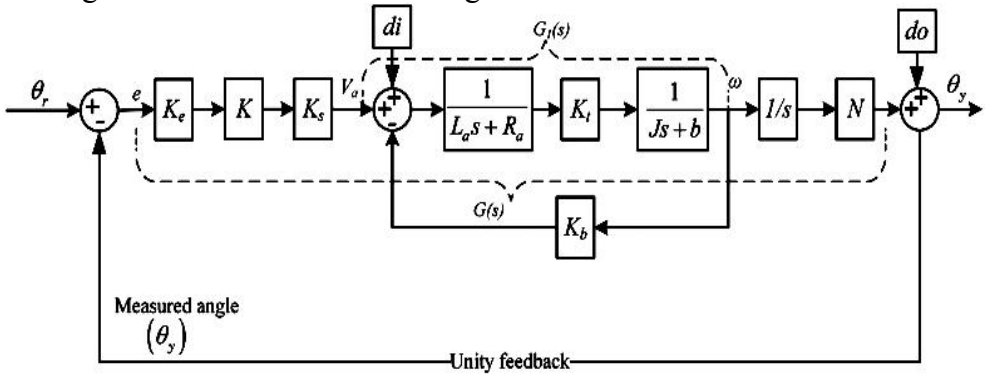

Figure 4.13: Model of solar tracking system

Figure 4.14 shows the Simulink block diagram of DC servo motor without controller.

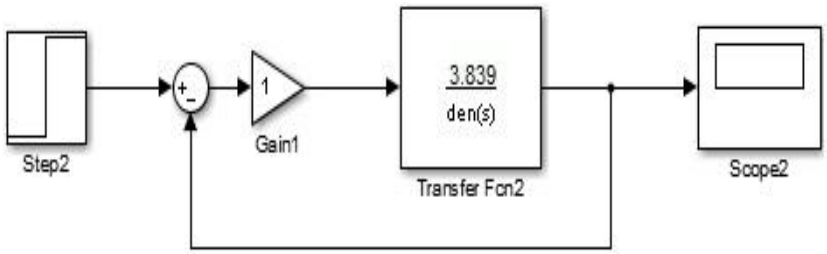

Figure 4.14: The Simulink block diagram of DC servo motor without Controller

The step response of DC servo motor without controller is shown in Figure 4.15.

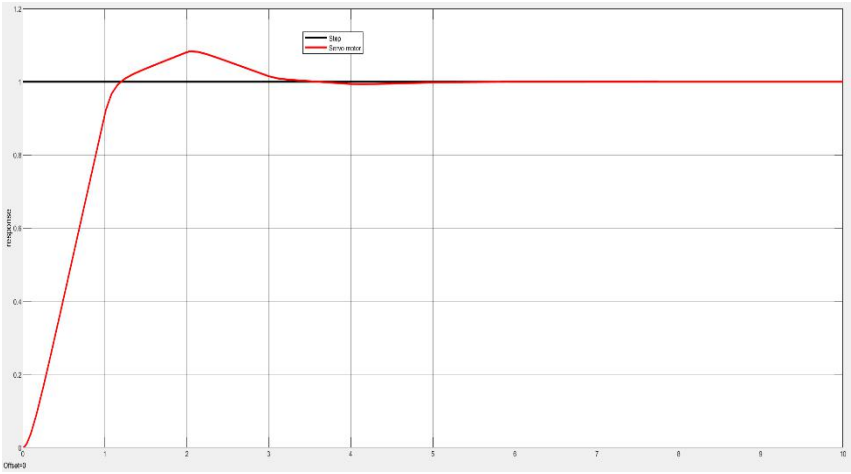

Figure 4.15: The response of DC servo motor without controller

4.4.1 Simulation result for PID controller

Figure 4.16 shows the Simulink block diagram of DC servo motor with PID controller (3.18). Furthermore, the step response of DC servo motor with PID controller is show in Figure 4.17.

The PID controller parameters is selected as K_p= 6, K_i= 0.06, K_d= 2.4.

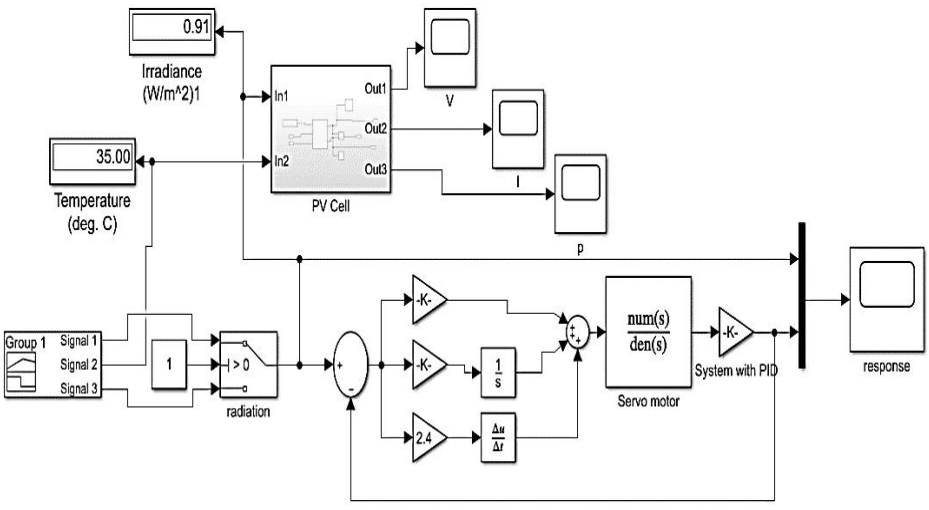

Figure 4.16: SIMULINK block diagram of DC servo motor with PID controller.

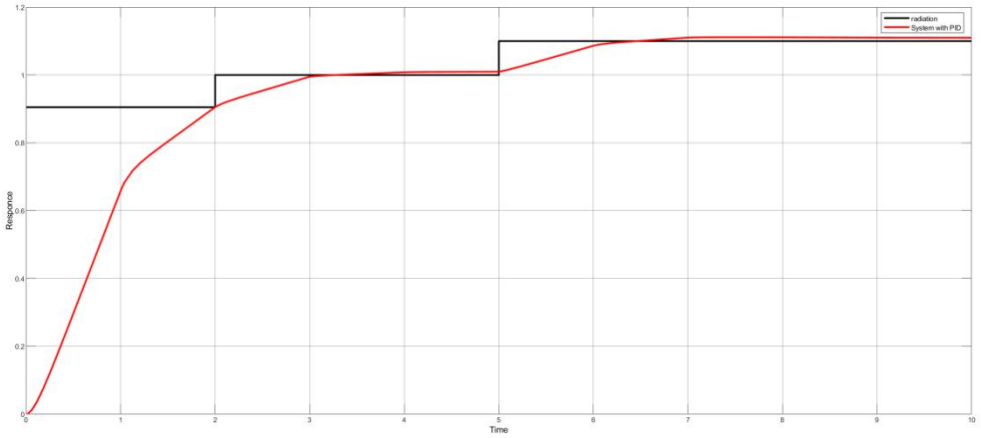

Figure 4.17: Step response of DC servo motor with PID controller

4.4.2 Simulation result for FOPID controller

Figure 4.18 shows the block diagram of dual axis solar taker with FOPID controller, Figure 4.19 shows the response of the system using FOPID controller and Table 4.2 and Table 4.3 shows the parameters of conventional PID controller.

Table 4.2: Parameters of conventional PID controller

PID	K_P=6	K_i=0.06	K_d=2.4

Table 4.3: Parameters of FOPID controller

FOPID	λ=0.9	μ =0.4

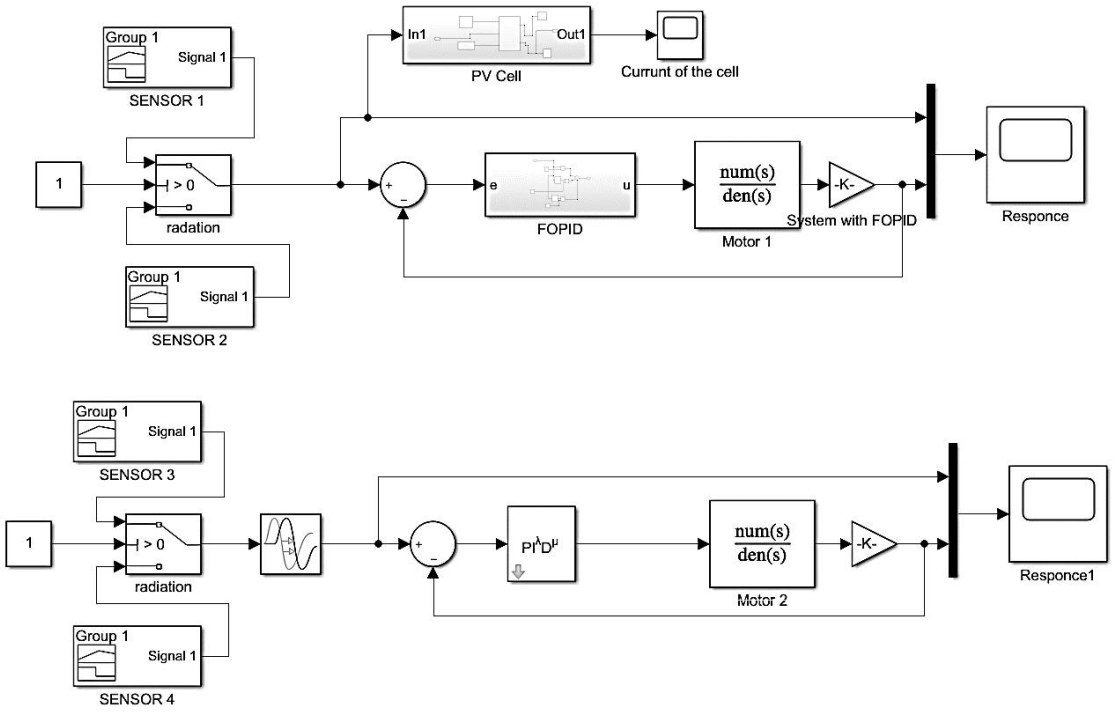

Figure 4.18: The block diagram of dual axis solar taker with FOPID controller

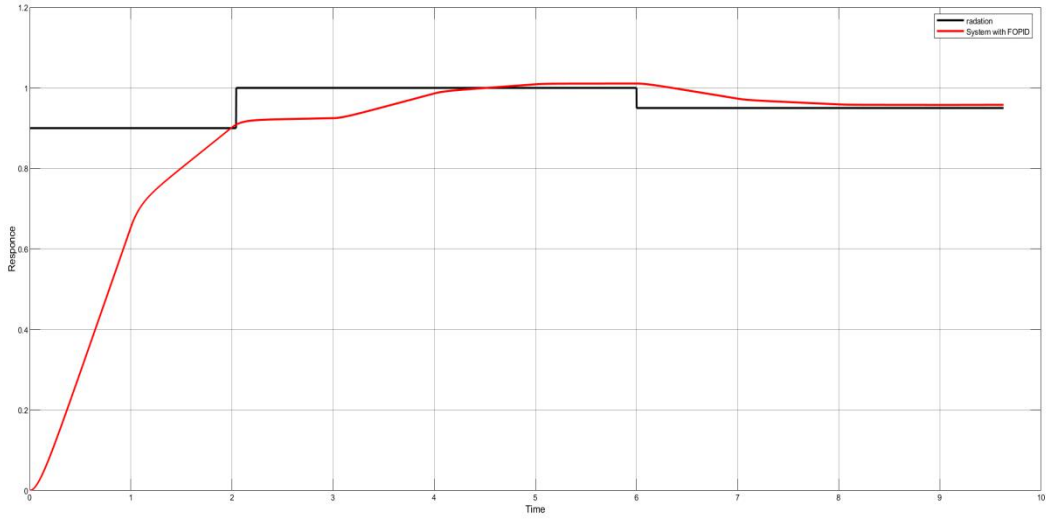

Figure 4.19: the response of the system using FOPID controller

4.4.3 Simulation of Dual Axis Solar Tracking System via FFOPID Controller

Figure 4.20 shows the response of the dual axis solar tracking system using Fuzzy Fractional Order PID Controller, Figure 4.21 shows the response of dual axis solar tracking system by using FFOPID controller and Table 4.4 shows the parameters of proposed controllers for dual axis sun tracker

Table 4.4: Parameters of proposed controllers for dual axis sun tracker

FFOPID	K_p range (0- 50)	K_i range (0 _ 50)	K_d range (0 _ 100)	$\lambda = 0.9$	$\mu = 0.4$

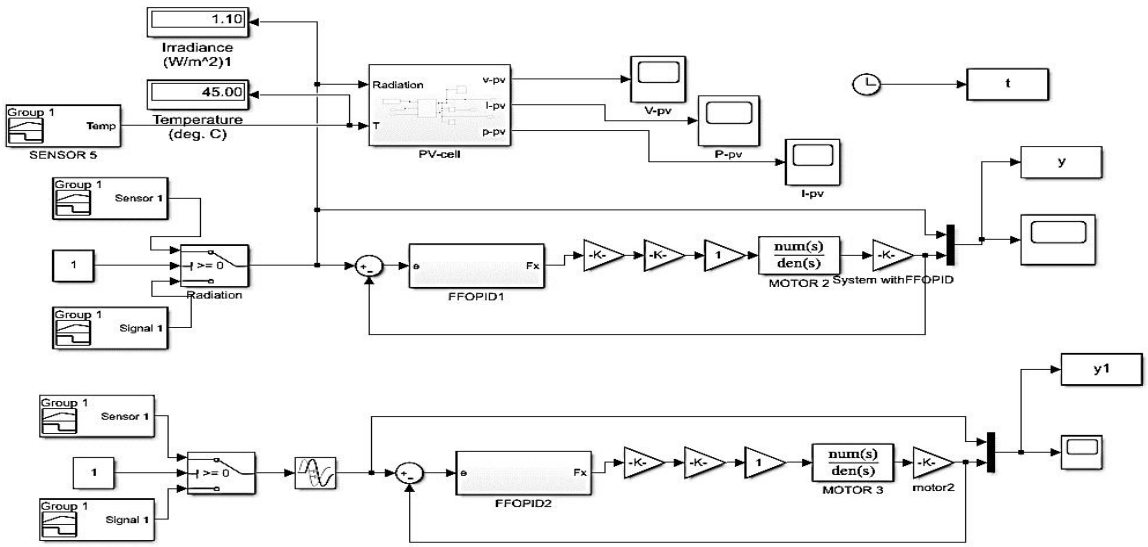

Figure 4.20: Block diagram of dual axis solar tracking system using FFOPID controller

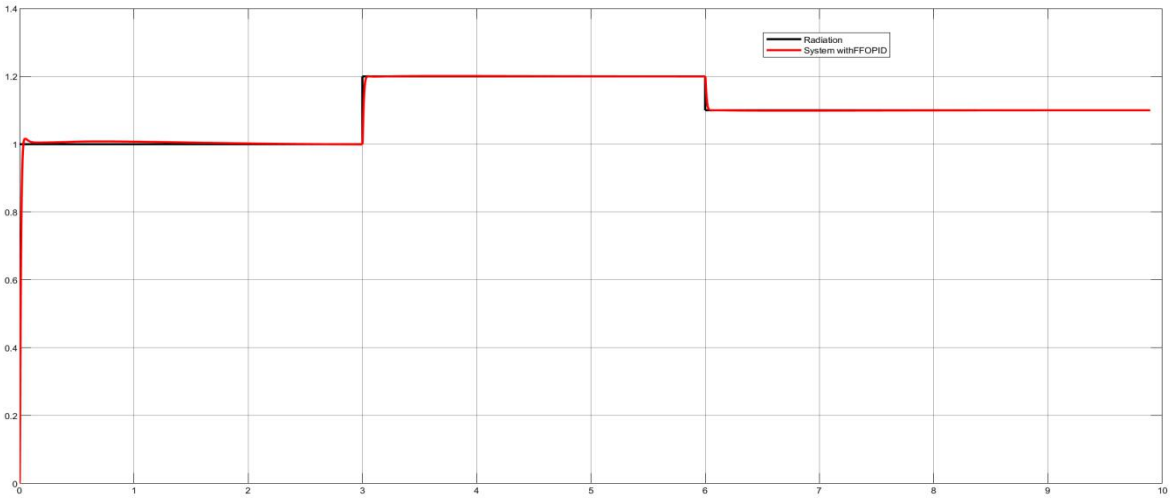

Figure 4.21: Response of dual axis solar tracking system by using FFOPID controller

4.4.4 Simulation of Dual Axis Solar Tracking System by using different types controllers

The proposed controllers are benchmark with a conventional PID and FOPID controllers to show the effeteness of the proposed controllers. Figure 4.22 and Figure 4.23 show respectively the block diagram dual axis Sun tracking system using PID, FOPID and FFOPID controllers and response of dual axis Sun tracking system using PID, FOPID and FFOPID controllers.

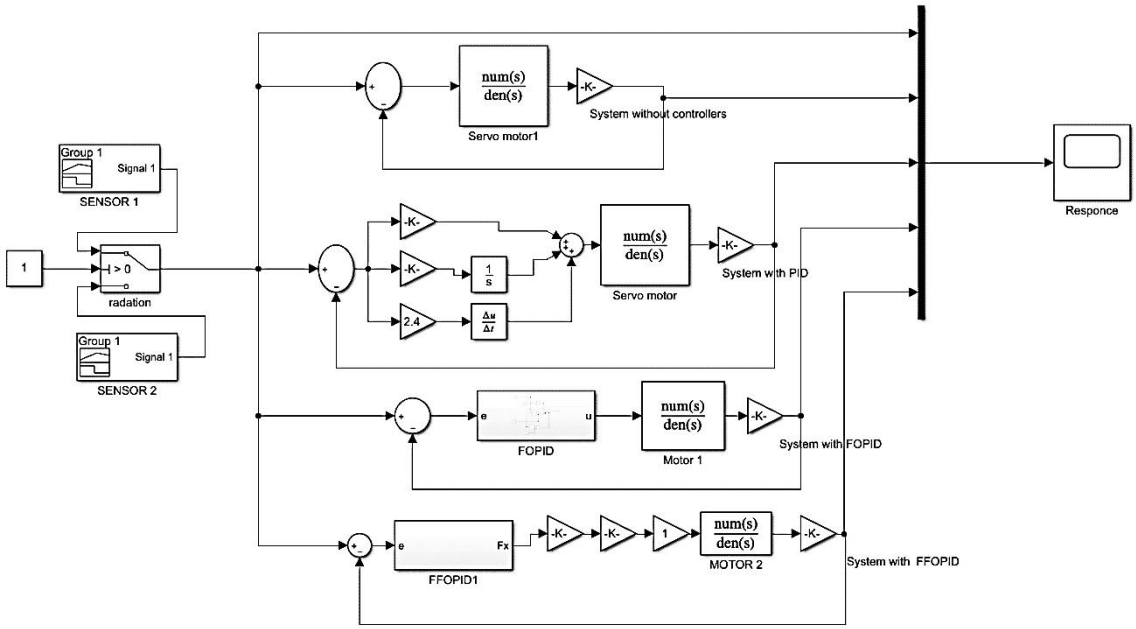

Figure 4.22: The block diagram of system by using PID, FOPID and FFOPID controllers

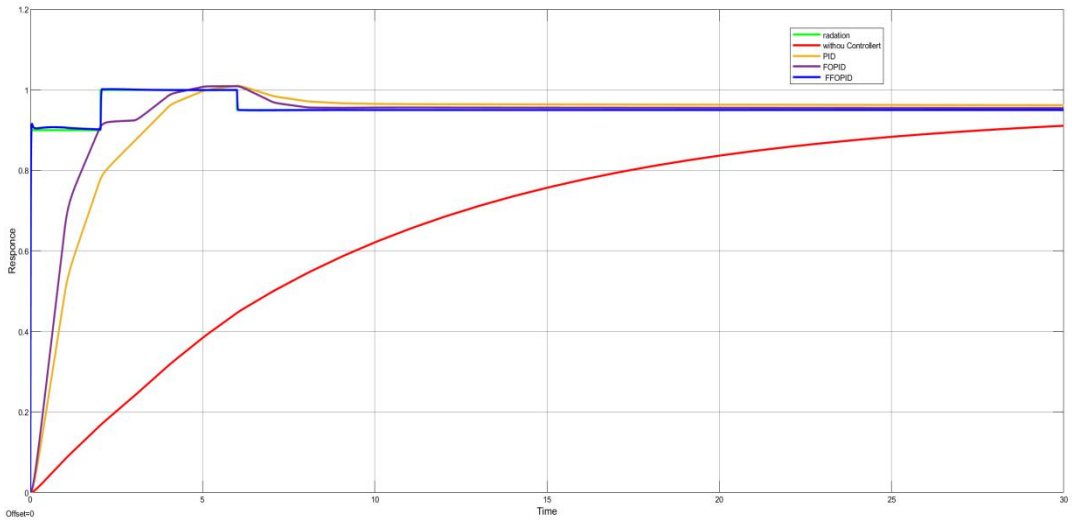

Figure 4.23: The response of system by using PID, FOPID and FFOPID controllers

4.5 Comparison the Result and Discussion

In order to validate the control strategies, digital simulation was carried out on a system. The MATLAB/SIMULINK models of system under study with the three controllers are shown in Figure 4.22.

The proposed FFOPID controllers are benchmarked with the results of a conventional PID and FOPID controllers as illustrated in Figure 4.23. The proposed FOPID has better transient response than the conventional PID controller; this is due to the flexibility added by fractional order parameters to adjust the output performance. Furthermore, the proposed FFOPID has a

faster response than PID and FOPID controllers, Therefore, the responses of the proposed controllers are superior to the conventional PID and FOPID controllers.

Table 4.5: Comparison between, maximums overshoot, rise times and settling time

Controller	Ts(sec)	Tr (sec)	Overshoot MP
PID	3.18	2.44	8.87%
FOPID	1.34	1.721	3%
FFOPID	0	0	0.9%

4.6 Summary

This chapter presented the simulation works of the dual axis Sun tracking system and PV model with the proposed FFOPID, FOPID and PID controllers and discussed the results. It's found that the results of the proposed FOPID are better than PID and FOPID controllers in reducing the transient response. Moreover, the proposed FFOPID has a faster response to track the radiation from the Sun.

CHAPTER FIVE

CONCLUSION AND RECOMMENDATIONS

5.1 Conclusion

Solar energy has become one of the important types of alternative energy sources, such reasons as accessibility, cost efficient in production and low-priced installation costs have made it favorable. However, one of the problems of solar energy technology is that needs to increase the solar panel output power.

The dual axis Sun tracking system had been maintained to get the maximum power output through utilizing the FFOPID control approach. The proposed controller is benchmarked with FOPID and conventional PID controllers. It's found that, the proposed controller is better than FOPID and PID controllers in terms of reducing the tracking error for both azimuth and tilt angle, which means achieving more power from the Solar panel through using FFOPID controller.

It is clear that form the simulation result the Performance of proposed FFOPID control for Sun tracking system better than PID and FOPID controllers in reducing the transient response. Moreover, the proposed FFOPID has a faster response to track the radiation from the Sun.

The results were benchmarked with the FOPID and conventional PID controllers. It's found that, the FFOPID reduced the transient response via 6.5% than FOPID and 9.6% than the conventional PID controller.

5.2 Recommendations

1. It is recommended that the system can be controlled by more advanced control techniques, like artificial neural network (ANN), genetic algorithm (GA), Particle Swarm Optimization (PSO), Ante Colony, Bee Colony.

2. Improve the response by modify the FFOPID controller to tune the fractional integration λ and the fractional derivative μ by using fuzzy logic.

3. Modify the FFOPID controller utilize robust control approach to enhance the result for uncertainty and external disturbance.

4. Impalement the proposed control approach experimentally.

REFERENCES

[1] M.J. Clifford, D. Eastwood, “Design of a novel passive solar tracker,” Solar Energy 77 (2004) 269–280.

[2] Daniel A Pritchard, “Sun Tracking by Peak Power Positioning for Photovoltaic Concentrator Arrays, IEEE, 1983.

[3] S. Budhy, P.H. Mauridhi, A. Mochama, H. Takashi, “Advance control of on-ship solar tracker using adaptive wide range ANFIS, “Int.J. Innov.Comput. Inf.Control9 (2013).

[4] M.J. Clifford, D. Eastwood, “Design of a novel passive solar tracker,” Solar Energy 77 (2004) 269–280.

[5] E. Lorenzo, M. Perez, A. Ezapeleta, J. Acedo,” Design of tracking photovoltaic system with a single vertical axis, Progress in Photovoltaic’s”, Research and Applications 10 (2002) 533–543.

[6] B.J. Huang, F.S. Sun, “Feasibility study of one axis three positions tracking solar PV with low concentration ratio reflector,” Energy Conversion and Management 48 (2007) 1273–1280.

[7] A. Yazidi, F. Betin, G. Notton, G.A. Capolino, “Low cost two-axis solar tracker with high precision positioning,” International Symposium on Environment Identities and Mediterranean Area- ISEIMA, 2006, pp. 211–216.

[8] T.A. Ocran, C. Junyi, C. Binggang, S. Xinghua, Artificial neural network maximum power point tracker for solar electric vehicle, Tsinghai Science and Technology 10 (2) (2005) 204–208.

[9] A.D. Karlis, T.L. Kottas, Y.S. Boutalis, “A novel maximum power point tracking method for PV systems using fuzzy networks (FN),” Electric Power Systems Research 77 (2007) 315–327.

[10] B.J. Huang, F.S. Sun, “Feasibility study of one axis three positions tracking solar PV with low concentration ratio reflector,” Energy Conversion and Management 48 (2007) 1273–1280.

[11] A. Yazidi, F. Betin, G. Notton, G.A. Capolino,” Low cost two-axis solar tracker with high precision positioning,” International Symposium on Environment Identities and Mediterranean Area- ISEIMA, 2006, pp. 211–216.

[12] J.L. Santos, F. Antunes, A. Chehab, C. Cruz,” A maximum power point tracker for PV systems using a high-performance boost converter,” Solar Energy 80 (2006)772–778.

[13] N. S. Nise,” Control systems engineering”. [Hoboken, NJ]: Wiley, 2004.

[14] K. Ogata,” Modern control engineering”. Englewood Cliffs, N.J.: Prentice-Hall, 1970.

[15] Leonid Rezink, "Fuzzy Controllers", Victoria University of Technology, 1997.

[16] Monje, Chen, Vinagre, Dingyü Xue, Vicente Feliu . “Fractional-order Systems and Controls Fundamentals and Applications”, Springer Verlag, London Limited, 2010.

[17] C. Y. Wang, "Study on Fractional Order PID Controller Parameter Tuning Method and Design", Jilin University, 2013.

[18] M.zadeh, H., Keyhani, A., Javadi, A., Mobli, H, (2009), “A review of principle and sun-tracking methods for maximizing solar systems output” in Renewable and Sustainable Energy Reviews, Tehran pp 1800–1818.

[19] M.M.Sabir , T.Ali, “Optimal PID controller design through swarm intelligence algorithms for sun tracking system “ , ELSEVIER Inc, University Institute of Information Technology,2015.

[20] S. Malik & S.K. Mishra “Optimal Design of a Fuzzy PID Controller for Inverted Pendulum System”, Springer India , 10.1007/978-81-322-2656-7_118, 2016

[21] D. Hanwate and V. Hote, “Design of PID controller for sun tracker system using QRAWCP approach”, International Journal of Computational Intelligence Systems, Vol. 11 (2018) 133–145.